ADDIS ABABA UNIVERSITY

ADDIS ABABA INSTITUTE OF TECHNOLOGY

SCHOOL OF CIVIL AND ENVIRONMENTAL ENGINEERING

A COMPARATIVE STUDY OF LIMITS ON NORMALIZED AXIAL LOADS OF ES-EN 1998:2015 WITH OTHER CURRENT MAJOR BUILDING CODES ON COLUMNS

A Thesis to the School of Civil and Environmental Engineering of Addis Ababa University Institute of Technology in partial fulfilment of the requirements of the degree of Master of Science in Civil (Structural) Engineering

By:

ABEL NEGUSSIE GORFU

April 2024

Addis Ababa, Ethiopia

The undersigned have examined the thesis entitled '**A Comparative Study of Limits on Normalized Axial Loads of ES-EN 1998:2015 With Other Current Major Building Codes on Columns**' presented by **ABEL NEGUSSIE**, a candidate for the degree of **Master of Engineering** and hereby certify that it is worthy of acceptance.

Dr. Adil Zekaria Advisor	Signature	08/04/2024 Date
Dr. Bedilu Habte Internal Examiner	Signature	Apr. 22/24 Date
Dr. Abrham Gebre Internal Examiner	Signature	April 8/2024 Date
Chair Person	Signature	Date

Director of Postgraduate Program
Addis Ababa University
Addis Ababa Institute of Technology

UNDERTAKING

I, undersigned **Abel Negussie** hereby declare that this thesis work titled **'A Comparative Study of Limits on Normalized Axial Loads of ES-EN 1998:2015 With Other Current Major Building Codes on Columns'** is my own work. To the best of my knowledge, this thesis contains no material previously published by any other author except where due acknowledgement has been made in accordance with the standard referencing practices.

Date: _____

Signature: _____

Abel Negussie

ABSTRACT

Axial loads highly affect the behavior of reinforced concrete members, such as failure mode, yield curvature, ultimate curvature, curvature ductility, beam-column joint, etc. In order to limit the adverse effects of axial loads, Ethiopian Standards based on Euro-Norms limits normalized design axial compressive loads. This research explores the basis for these limits and then compares them with other major codes and standards. The primary aim for these limits is for the axial loads not to exceed loads at balanced failure, v_{bal}. To study the balanced conditions, a series of $v - \mu$ interaction charts were constructed with the confinement effect of transverse reinforcement on concrete considered. The three main parameters for the charts are the distance of compression reinforcement from the extreme compression fibres normalised with respect to effective depth, $\delta_1 = d_1/d$, mechanical reinforcement ratios, ω, and mechanical volumetric ratio of confining reinforcement, ω_ω. Sectional properties, i.e., yield curvature, ultimate curvature and curvature ductility, under the obtained balanced axial loads were compared to their perspective limits. It was concluded that v_{bal} is highly affected by δ_1, and to a lesser extent by ω and ω_ω. It has an inversely proportional relationship with both δ_1, and ω. Fifteen different column section was also considered as an example, and their results are in alignment with the $v - \mu$ interaction charts. From the results obtained, it can be concluded that the limits can be more directed for values of δ_1. This is especially the case for column sections having lower values of δ_1 which show a greater load capacity than the set limits.

Table of Contents

Table of Figures

Notations

A_c, A_g: is the cross-sectional area of the concrete

A_{st}, A_{sc}: total area of non-prestressed longitudinal reinforcement.

E_c, E_s: modulus of elasticity of concrete and reinforcement

f_{cd}: the design compressive strength of concrete

$f_{ck}, f_c', f_c, f_{cu}$: characteristic compressive strength of concrete,

$f_{ck,c}$: confined compressive strength of concrete

f_y yield strength of reinforcement,

N_{Ed}: is the design axial force

M_{Ro}, M_{Rc}: moment resistance of the confined core and of the un-spalled section

b, h: width and height of a cross-section

d: effective depth of a section

Greek

ρ_w is the volumetric ratio of confining reinforcement

ρ: reinforcement ratio

ω_w is the mechanical volumetric ratio of confining reinforcement

ω: mechanical volumetric ratio of longitudinal reinforcement

ξ_y, ξ_u: normalized neutral axis depth at yield and ultimate state

φ_y, φ_u: curvature at yield and ultimate state

μ_φ: curvature ductility

ν: normalized axial load

μ: normalized moment

γ_c, γ_s: partial factor for concrete and steel

δ_1: normalized distance of the compression reinforcement from the extreme compression fibres

$\varepsilon_{co}, \varepsilon_{co,c}$: compressive strain of unconfined and confined concrete at the peak stress

$\varepsilon_{cu}, \varepsilon_{cu,c}$: ultimate compressive strain of unconfined and confined concrete

ε_y: yield strain of reinforcement

ε_{su}: characteristic strain of reinforcement

Acknowledgements

This work would not have been possible without the financial support of Ethiopian Road Authority Scholarship, and my appreciation for providing the opportunity to all students like myself.

This paper and the research behind it would not have been possible without the exceptional support of my supervisor, Adil Zekaria Ph.D. His enthusiasm, knowledge, and exacting attention to detail have been an inspiration and kept my work on track from the proposal to the final draft of this paper.

I am especially indebted to my boss and mentor Eng Yibeltal Zewdu, who has been supportive of my career goals and who worked actively to provide me with the protected academic time to pursue those goals.

I would like to thank my parents; whose love and guidance are with me in anything I pursue. They are the ultimate role models.

Last but certainly not least, I would also like to express my immense gratitude to all my friends and everyone who helped me in my journey.

CHAPTER 1: INTRODUCTION

1.1. General

Modern seismic design codes around the world recognize the importance of ductility as it plays a vital role in structural performance against earthquakes. Ductility relates action and corresponding deformation. It can be analyzed at several levels; at structural level: Load-Deflection, at member level: Moment-Rotation, at cross-sectional level: Moment-Curvature and at Material level: Stress-Strain. All of these relations are highly influenced by the presence of axial force. This paper will examine the effect of axial loads on ductility at the cross-sectional, i.e., yield curvature, φ_y, ultimate curvature, φ_u, and curvature ductility, μ_φ.

Under intense seismic actions, columns have fluctuating axial loads. Many books and papers have suggested for higher levels of compressive axial load (ACL), there is an adverse effect on the section's stiffness, ultimate strength and even its mode of failure (brittle or ductile failure). This is especially the case if the value of axial force varies around balance load, as there is no clear-cut effect of the variation on the column flexural behavior [1].

To address this effect, Ethiopia Standards based on Euro-Norms (ES-EN 1998:2015) [2] along with Eurocode 8 [3] have set limits on normalized axial force ratio, v, for different ductility classes. Whereas, American Concrete Institute (ACI 318) [4] sets no such limits.

1.2. Problem Statement

When designing a new reinforced concrete structure according to requirement of ES-EN 1998:2015, let us say a column member fails to meet the limits of normalized axial compressive load. For the column to pass these limits, its design compressive strength needs to be enhanced. Generally, there are two ways to do this. The first way is to increase the compressive strength of concrete by using a higher concrete grade. The second option is to increase the cross-sectional dimension of the column. The latter option will result in columns having larger cross-section, often negatively interfering with the intended architectural functions.

The limit stipulated by our code only take in to account the concrete compressive strength and neglect the contributions of the reinforcements. *Why?* Confinement effect, enhancing strength of concrete is also ignored. Again, *why?*

There is no clear consensus among different design code; on wheatear or not to limit the value of v, nor is there common agreement on how the limits are expressed. In this study, these problems will be explored.

1.3. Objective of the Study

General Objective

- To research if there are any other similar stipulation by other design codes
- To perform comparative research on the limits of codes having similar limitations
- To explore the origins, necessity, and the basis of these limits

Specific Objective

- To plot a series of normalized $v - \mu$ interaction charts
- To obtain the normalized axial compressive load at balanced failure point
- To conduct a parametric study on the selected three variables to explore their effects on the value of balanced load failure
- Present example case studies

1.4. Scope of the study

- This study is limited to researching six major design codes
- No laboratory experiments were done to verify or validated the data
- Curvature ductility is the only selected variable for measuring any changes in ductility

1.5. Methodology

The limits on normalized axial compressive load on column stipulated in ES-EN 1998:2015 was compared with other major, current, and relevant design codes of other countries. After these comparisons was made, an investigative study was commenced to explore the origins of the limits of ES-EN 1998:2015. Once the reason behind setting these limits was found, the values of normalized axial compressive load at balanced failure point for different possible conditions was studied. This was done by plotting a series of normalized $\nu - \mu$ interaction charts.

Three main varying parameters were selected to best represent all the possible cross-section that one may run in to on a day-to-day basis. These parameters considered are the distance of compression reinforcement from the extreme compression fibres normalised with respect to effective depth, $\delta_1 = d_1/d$, mechanical reinforcement ratios, ω, and mechanical volumetric ratio of confining reinforcement, ω_ω. The two values of confinement considered are adjusted so that they meet the minimum requirements of medium and high ductility classes of ES-EN 1998:2015.

After the balanced axial load is calculated, the curvature ductility of the cross-section at the balanced failure point was compared to its respective ductility under the stated limits of axial loads. This was done to see if there is any significant loss in ductility. Finally, fifteen sections were presented as an example case studies.

Further detailed explanation of the methodology followed by this paper is presented in Chapter 3.

1.6. Organization of the Study

This study consists of five chapters with additional three annex.

The first chapter presents an introduction to the subject matter by discussing the background, the statement of the problem, the objective, scope, methodology, and organization of the thesis.

In Chapter 2 a comprehensive look at previous literatures similar to this study can be found. The papers were selected based on their degree of relevance to this research. Major seismic design codes can also be found in this part.

Chapter 3 shows a detailed explanation on the methodology followed by the study. The material properties, along with the influenced of confinement on them, specifical on concrete. Moment curvature and curvature ductility relation at yielding is further explored. Results and Discussions are shown in Chapter 4.

Chapter 5 summarizes the findings of the research. The literature review, key observations and discussions are also compiled. Finally, recommendations are made, as well as suggestions for further study.

Annex A presents a detailed procedure for calculate and plotting the axial-load-moment interaction charts, while these charts are shown in Annex B. Verification of the new chart with the existing design charts of ES EN 1992:2015's Design Aid can be found on Annex C.

CHAPTER 2: LITERATURE REVIEW

Besides confinement detailing and axial loads, the ductility and general seismic performances of RC columns can be influenced by various factors, such as the anchorage, loading pattern, etc., of which effect in turn interact with confinement and axial load effect.

Axial compression loads discussed here should not be confused with the limit state design concepts, since the axial compression ratio alone cannot represent the state of a member nor can it be used to assess the actual seismic performances of the RC members. Assessing the actual seismic responses of the RC columns under significant axial force can be complex, as there are lots of interdepending parameter that influence one other.

Knowing this, there is a clear vested interest to investigate the effect of axial load on the performance and behavior of RC buildings. Although there are several books, experiments, journals and papers that are aimed at studying the effect of axial load on the ductility and flexural behavior of a reinforced concrete section, most of the experimental tests were carried out under comparatively low levels of axial load.

Some of the major effects of axial load are discussed here in.

2.1. Effect of Axial Load on Ductility

High magnitude earthquake imposes large deformations that might be well beyond the elastic limits of the structure. The ability of the structure and its components, or of the material used to offer resistance in the inelastic domain of the response, is described by the general term ductility [5]. In other words, ductility is the ability of a structure or structural members to deform beyond elastic limits without excessive strength or stiffness degradation. Ductility can be evaluated at many levels, such as strain, curvature, rotation or deflection. The main focus of this paper will be limited to curvature ductility.

On a section level, the presence of axial force significantly affects curvature ductility of the section. Generally, axial compression increases the yield curvature, φ_y, and decreases the

ultimate curvature φ_u, thus decreasing the available curvature ductility capacity of a section. On the contrary, the presence of axial tension increases ductility capacity.

Yet, on a member level the realistic relation between axial load and ductility is far more complex, owing to the fact that various factors, including axial force, aspect ratio, stiffness, cracks, etc... can interact with one another resulting in complex overall structural behavior.

The displacement ductility factor is also commonly used to assess the behavior of members. The displacement ductility in columns is closely related to the curvature ductility. However, for a column under high axial load with large $P-\Delta$ effect, displacement ductility might not be the best parameter to judge the ductility of columns.

With the aim to evaluate and quantify the effect of axial compression ratio (ACR) on the structural performance of RC columns and structural walls, and to investigate limits on ACR set by various design codes, commenced an analysis on 474 sets of experimental data [6-9].

The statistical analysis reveals that the ductility, ultimate displacement, drift capacity and hysteretic dissipation capacities of the flexure-critical RC columns under cyclic loading can be significantly reduced by increasing ACR, although the lateral strength shows a reversed trend. On the contrary, the displacement ductility of short columns is apparently not influenced by ACR, yet their ultimate drift ratio and hysteretic dissipation capacity deteriorates under high ACR.

The results also suggest that different ACR limits should be used for the design of slender and short columns due to different failure mechanisms. EC8 sets reasonable limits to the AFR for RC columns designed to different ductility classes, yet different limits should be used for slender and short columns as they are controlled by completely different failure mechanisms.

For typical flexural-controlled columns with confinement $\omega_v > 0.1$, a suitable AFR limit can be taken as ≤ 0.50. However, for shear-controlled columns the ultimate drift capacity shall not be less than 0.02% of the column height and the ACR limit is tightened up to ≤ 0.40.

For slender walls, there was a trend of diminishing ultimate displacement capacity with an increase in axial compression ratio owing to the reduction in neutral axial depth, low cycle fatigue effect as well as potential out-of-plane buckling. For squat wall with aspect ratios (H/L) greater than 1.5, shear strength and sliding resistance of cracks are enhanced by axial compression. This effect is reflected by an enhanced ultimate displacement capacity increases with increasing axial compression ratio[9].

The relation curve of displacement capacities and ACR tends to converge to the same value of ductility or ultimate displacement regardless of the level of confinement detail. The diminish in effectiveness of confinement on enhancing the displacement capacity at high level of ACR, clearly indicate the need for limiting ACR.

It is shown that a quite drastic drop in the displacement capacities following the increase of ACR from 10% to 30%, after where the relationship curves become stagnating and tend to converge to the same value of ductility or ultimate displacement, thus the confinement details become irrelevant thereafter.

Further investigation on drift ductility and axial force indicated that high ductility in RC wall can be achieved at low axial force ($v \leq 0.10$) so long as the boundary elements are well designed and detailed. When the axial compression ratio exceeds 0.20, only moderate ductility can be attained, with failure caused by pre-emptive out-of-plane buckling for $v > 0.35$. Compared to slender RC walls, the ductility of squat RC walls is less influenced by axial compression ratio.

2.2. Effect of Axial Load on Beam-Column Joints

Axial load ratio significantly influences the seismic behavior of beam-column joints, depending on the level of shear and bond of crossing portion beam and column reinforcement.

There are two distinct stages of mechanical behavior of joints [10]. The first stage is marked just before severe bond deterioration of the crossing portion of beam reinforcement occurs. The hoops carry the diagonal tension after diagonal cracks are formed. Forces of reinforcement in the joint transferred by bond effect decreases upon further bond deterioration. This designates the

final stage. At this stage damage of the joint accumulates as cracks along two diagonals of the joint core open and close alternately, and number of cracks increases. At second stage the role of hoops is mainly to confine the concrete.

To explore this 10 interior beam-column subassemblies with different levels of shear and axial forces to cyclic loading [10].

Owing to the decrease in the penetration of yield of the beam reinforcement into the joint core, bondage deterioration and crack formation will be delayed as axial load ratio increases. For joints under moderate or high shear, they still serious causing the concrete core to crush in the final stages, even though its delayed. This however is not the case for smaller shear. Overall favorable effect remains as a whole with no significant unfavorable effect on the second stage

It was concluded, while an increase in axial load ratio is favorable to energy dissipation capacity of joints with small shear, unfavorable effect is noticed on the joints with high shear, resulting in premature shear failure, that is, crush of the joint core concrete.

2.3. Effect of Axial Load on Shear Resistance of Columns

With the goal of obtaining data about the behavior of columns at deformations beyond those that cause them to lose their ability to carry gravity loads, two lightly reinforced shear-critical columns were experimentally subjected to high levels of axial load and lateral load reversals [11]. These types of columns, whose lateral load capacities are limited by their shear strength, are most vulnerable to sudden axial failure.

Although both columns had a brittle behavior, the results show, for higher drift demand the two columns had a significantly different behavior. For example, axial load stably carried by the columns after the first failure event was significantly lower for column under lower axial load.

The lateral stiffness and the residual axial load capacity of the columns were found to be related to the axial load prior to axial failure. For column with higher axial load, the lateral stiffness of the column after the first failure event was negligible. While for column with lower axial load,

lateral stiffness continued to decrease until it became negligible, at which point a second failure event was triggered.

The observation mentioned above were carried out pseudo-static tests. In real structures, however the ability of the column to continue to deform with reduced capacity will be dependent on the diaphragm action of the floor system.

Another important structural property explored was shear strength of RC walls, examined through the relationship between normalized shear strength and axial compression ratio. It was concluded, higher axial compression enhances not only the shear strength of shear walls but for some cases moment resistance also [9]. However, as the ductility of the system is of the utmost importance, it was clearly noted that the enhancement caused by axial load cannot outweigh its adverse effect of drift capacity.

Given the evidently poor seismic performances, shear-controlled columns should be avoided. If shear columns are inevitable, the ultimate drift capacity shall not be less than 0.02% of the column height and the AFR limit is tightened up to ≤ 0.40 in order to guarantee life-safe performance level [6]. For typical flexural-controlled columns with confinement $\omega_v > 0.1$, a suitable AFR limit can be taken as ≤ 0.50.

2.4. Effect of Axial Load on Confinement Requirements of Columns

In the modern seismic design, the properties of RC columns such as, the ultimate displacement, ductility and energy dissipation capacity are highly improved by concrete confinement in the potential plastic hinge regions with transverse reinforcement.

The required quantity of confining reinforcement is largely dependent on the level of axial compression induced onto the columns. The effectiveness of typical detailing for concrete confinement is often deteriorating with increase of axial compression and therefore many modern seismic design codes also stipulate upper limits on axial compression ratio.

In particular after $AFR > 0.50$, increasing amount of confining reinforcement is no longer as effective in enhancing the drift capacity as it is in the low AFR level [6]. Yet, the lateral strength increases with increasing AFR.

2.5. Code Provisions on Normalized Axial Loads

The requirement imposed by modern seismic codes and standards, for design of new buildings and retrofitting of existing structure, are aimed at protection of life and property under earthquake. Generally, these requirements will result in a building able to resist a moderate earthquake with insignificant structural damage, while resisting major earthquakes with some structural damage without collapsing. These requirements give rise to "Performance-based earthquake engineering", which first came about in the SEAOC Vision 2000 document and developed into the single most important idea of recent years for seismic design or retrofitting of buildings (SEAOC 1995).

These provisions, in general, consist of four requirements: (i) capacity design provisions to achieve a hierarchy of strength in order to avoid brittle failure modes, (ii) provision of special confining reinforcement (in the form of closely-spaced stirrups) at potential plastic hinge locations, (iii) anchorage of beam longitudinal reinforcement into columns, and (iv) design of beam-column joints to avoid shear failure

These requirements and design rules are provided in the new Ethiopian Standard based on Euro-Norms Part 1, ES-EN 1998:2015 Part 1-1 [2]. As the title implies our code is based on Eurocode – 8 Part 1-1 [3]. Their equivalence for US are given in American Concrete Institute ACI 318-11 [4], while for New Zealand is NZS 3101: Part 1: 2006-A1&A2 [12], for People's Republic of China it is GB 50011-2010 Code for Seismic Design of Buildings [13], for Hong Kong its Code of Practice for Structural Use of Concrete 2013 [14]. As the title of the paper indicates, the main focus of this study will only be to compare the limits provision on normalized axial load, if any, on these codes.

Most Modern seismic code appropriate combination of strength and ductility depending on seismicity of the site, the importance and occupancy of the building and other design parameters.

ES-EN and ACI provided discrete strength-ductility combination, available for the designer to choose from. Each one with its own well-defined rules for member dimensioning and detailing.

i. Ethiopian Standard based on Euro Norms (ES-EN 1998:2015) & Eurocode-8

ES-EN 1998:2015 [2] allows a building to be designed and detailed for three Ductility Classes (DCs), which are Ductility Class Low (DCL), Ductility Class Medium (DCM) and Ductility Class High (DCH). Each ductility class has its own set of requirements and detailing to be met for a structural member.

Buildings designed for DCL are not specially detailed to be ductile, but do possess a certain minimum ductility specified in ES-EN 1992:2015 [15]. DCM and DCH are subjected to a more stringent detailing requirements for members. There are no limits on normalized axial load ratio, for DCL. Whilst the limits for normalized axial load ratio caused by seismic action, for DCM and DCH are 0.65 and 0.55 respectively.

$$v = \frac{N_{Ed}}{A_c f_{cd}} \leq \begin{cases} - & \rightarrow DCL \\ 0.65 & \rightarrow DCM \\ 0.55 & \rightarrow DCH \end{cases} \tag{2.1}$$

where; N_{Ed} is the design axial force, A_c is the cross-sectional area of the column and f_{cd} is the design compressive strength of concrete.

In Eurocode 8 [3], which is the basis for ES-EN, stipulates the exact limits for the same ductility classes. These limits were based on the work by Chronopoulos and Vinzileou (1995), despite the largely scattered results [9].

ii. American Concrete Institute, ACI 318-11

ACI classifies buildings into three groups. These are “Ordinary Moment Frames”, “Intermediate Moment Frames”, and “Special Moment Frames” [4]. Similar to ES-EN, each class has its own

set of requirements and detailing to be met for a structural member. ACI sets no specific limitation for the axial load ratio for seismic action, but does have one for all column members regardless of earthquake action. This limitation is dependent not only on the nominal axial compressive strength of columns as in the non-seismic design, but also dependent on the amount of longitudinal reinforcement, cross-section and confinement type used.

Nominal axial compressive strength P_n shall not exceed $P_{n,max}$, where $P_{n,max}$ is $0.80P_o$ and $0.85P_o$ for spiral and tie confinements respectively. The nominal axial strength at zero eccentricity, P_o, is given by

$$P_o = 0.85f_c'\left(A_g - A_{st}\right) + f_y A_{st} \tag{2.2}$$

Where: f_c' is specified compressive strength of concrete, f_y yield strength of reinforcement, A_g is gross area of concrete section, A_{st} is total area of non-prestressed longitudinal reinforcement. Strength reduction factor, ϕ, has different value; for compression-controlled section: $\phi = 0.75$ for spiral reinforcements, and $\phi = 0.65$ for other reinforced member.

iii. NZS 3101.1.2006

New Zealand (NZ) has two limits on maximum design axial load in compression, N_o^*, on columns and piers: for members designed for ductility in earthquake N_o^* shall not exceed $0.7N_{n,max}$, and for non-seismic columns N_o^* shall be less than $0.85N_{n,max}$. Where $N_{n,max}$ is

$$N_{n,max} = \alpha_1 f_c'\left(A_g - A_{st}\right) + f_y A_{st} \tag{2.3}$$

Where: N_o^* is the design axial load derived from overstrength considerations (capacity design) (N),

$N_{n,max}$ is the nominal axial load compressive strength of column when the load is applied with zero eccentricity in N,

α_1 is a factor that takes in to account equivalent rectangular concrete stress distribution, $\alpha_1 = 0.85$ for concrete strength up to and including $55\,MPa$, and for strength above it $\alpha_1 = 0.85 - 0.004(f_c' - 55) \geq 0.75$,

f_c' is specified compressive strength of concrete in MPa,

f_y is lower characteristic yield strength of non-prestressed reinforcement or the yield strength of structural steel casing in MPa,

A_g and A_{st} are gross area of section and total area of longitudinal reinforcement respectively both in mm^2

iv. Code for Seismic Design of Buildings (GB 50011- 2010)

Based on GB 50011-2010 [13] RC members can be design and detailed by one of the four seismic structural grades, and they are noted as Grade 1-4. Each Grade has its own set of rules, Grade 1 being the most stringent requirements and detailed to meet high ductility. For moderate seismic action, it recommends Grade 2 or 3. For low ductility requiring members Grade 4 is advised.

This code sets a limiting value on the axial-force-ratio of columns for the previously mentioned grades, along with the type of structure to be designed. The axial-force-ratio limits shown in Table-1, refers to the ratio of the design axial compressive force (including seismic effects) value to the product of the column cross-sectional area, A_c, and the design compressive strength of concrete, f_c. Contrary to all the other codes examined here, this code also requires the necessity of these limits for structures that are not checked for earthquake. However, design axial compressive force calculated is without seismic effects.

GB 50011-2010: Code for Design of Concrete Structures [16], gives the values for f_{ck} and f_c, which are the characteristic and design value of the axial compressive strength of concrete respectively, in a table format. The relation between them, i.e., f_{ck}/f_c, has an average value of 1.40, although it depends on the strength of concrete. The value listed for f_c in the table is again adjusted by correction coefficient of fatigue strength, γ_ρ. This factor takes into account the minimum and maximum stresses of concrete at the same fiber of the section in fatigue analysis of members.

Table 2-1 Limit Value for the Axial-force-ratio of Column (GB50011-2010)

Type of Structure	Seismic Grade			
	1	2	3	4
Frame Structure	0.65	0.75	0.85	0.90
Frame-seismic wall, slab-column-seismic wall, frame-core-tube, tube-in-tube	0.75	0.85	0.90	0.95
Frame-support seismic wall	0.60	0.70	-	-

Frame structure type will be considered for comparison with ES EN 1998:2015.

v. Code of Practice for Structural Use of Concrete 2013 (Hong Kong)

Hong Kong's concrete code does not take seismic load in to consideration in any of its required load combinations. It has a restricting limit, N, on design ultimate axial load of columns for two conditions.

For uniaxial short columns: $N = 0.4f_{cu}A_c + 0.75A_{sc}f_y$

For short columns supporting an approximately symmetrical arrangement of beams: $N = 0.35f_{cu}A_c + 0.67A_{sc}f_y$

Where: f_{cu} is characteristic compressive strength of concrete, f_y characteristic yield strength of reinforcement, A_c is gross area of concrete section, and A_{sc} is area of longitudinal reinforcement (it denotes main reinforcement in column, wall or pile and does not necessarily imply that the reinforcement will be in compression.).

CHAPTER 3: METHODOLOGY

It is very clear the need to explore the effect of axial load, especially axial compression loads due to seismic action. This chapter outlines the procedure followed to investigate these effects.

The first step is to define the behavior of the materials that makeup a reinforced concrete section.

3.1. Characteristics of Material

A reinforced concrete column is made up of, as the name implies; concrete which is reinforced both in the longitudinal and transverse directions by steel. Therefore, to understand the behavior of RC columns, it is paramount to study the stress-strain ($\sigma - \varepsilon$) relationship of both materials, concrete and steel, under varying conditions.

3.1.1. Numerical Models for Concrete

The concrete in columns confined with transverse reinforcement consists of unconfined (cover) and confined (core) concrete. These two parts behave essentially the same at first instance of loading, but differ greatly after the ultimate strain is reached. As such it will be best if the model for concrete be separated into two, and they will be discussed as follows.

3.1.1.1. Numerical Models for Unconfined Concrete

In this paper the behavior of unconfined concrete is described, as per ES-EN 1992:2015; having a parabolic $\sigma - \varepsilon$ curve until an ultimate strength of f_{ck} and a corresponding strain, ε_{c2} is reached. After which, $\sigma - \varepsilon$ remains horizontal for strain less than the ultimate strain, i.e., $\varepsilon_c \leq \varepsilon_{cu2}$. Since the concrete classes used in this paper are all less than $C50/60$, the previous statement can be mathematically expressed as

$$\sigma_c = \begin{cases} f_{ck}\left(1 - \left(1 - \frac{\varepsilon_c}{\varepsilon_{c2}}\right)^2\right) \rightarrow for\ 0 \leq \varepsilon_c \leq \varepsilon_{c2} \\ f_{ck} \rightarrow for\ \varepsilon_{c2} \leq \varepsilon_c \leq \varepsilon_{cu2} \end{cases} \quad (3.1)$$

Where: σ_c is the compressive stress in the concrete, f_{ck} is characteristic compressive cylinder strength of concrete at 28 days. ε_c, ε_{c2}, and ε_{cu2} are compressive strain in the concrete, compressive strain in the concrete at the peak stress f_{ck}, and ultimate compressive strain in the concrete, respectively.

3.1.1.2. Numerical Models for Confined Concrete

The ductility of concrete is enhanced when adequately confined. Confinement in columns can come from transverse reinforcement, like closely placed hoops or ties, and Fibre-Reinforce Polymers (FRPs). Confinement by transverse bar will be the only focus of this study.

The effectiveness of rectangular or square hoops, although not as effective in confining as spiral or circular hoops, can significantly be improved by using overlapping hoops or with crossties

The way adequately placed transverse bars affect ductility of concrete is quite simple. They, along with longitudinal bars, oppose the lateral Poisson expansion of the concrete due to a compressive stress, σ_1, acting along the main axis of the member. This expansion exerts a tensile stress, σ_2 and σ_3, in the hoops causing the core concrete to be in a triaxially compressed state. As the concrete reaches its ultimate strength, a uniform confining pressure, $\sigma_2 = \sigma_3 = p$, at right angles to σ_1, increases the compressive strength in the direction of σ_1 from f_{ck} to $f_{ck,c}$ and more importantly the strain at the peak of the $\sigma_1 - \varepsilon_1$ curve from ε_{co} to $\varepsilon_{co,c}$.

ES-EN 1992:2015-1-1 3.1.9(2) gives the formula for $f_{ck,c}$, $\varepsilon_{c2,c}$ and $\varepsilon_{cu2,c}$ as

$$f_{ck,c} = \begin{cases} f_{ck}(1.000 + 5.0\,\sigma_2/f_{ck}) \ \rightarrow for\ \sigma_2 \leq 0.05 f_{ck} \\ f_{ck}(1.125 + 2.5\,\sigma_2/f_{ck}) \ \rightarrow for\ \sigma_2 > 0.05 f_{ck} \end{cases} \quad (3.2a)$$

$$\varepsilon_{c2,c} = \varepsilon_{c2}\left(f_{ck,c}/f_{ck}\right)^2 \quad (3.3a)$$

$$\varepsilon_{cu2,c} = \varepsilon_{cu2} + 0.2\,\sigma_2/f_{ck} \quad (3.4a)$$

Where: $f_{ck,c}$ is characteristic confined compressive cylinder strength of concrete, $\sigma_2 (= \sigma_3)$ is the effective lateral compressive stress at the ULS due to confinement. $\varepsilon_{c2,c}$ and $\varepsilon_{cu2,c}$ are the confined compressive strain at the peak stress $f_{ck.c}$ and confined ultimate strain, respectively.

However, ES-EN 1998:2015 Part-3 for the assessment and strengthening of existing structure, has adopted the value of K proposed in (Newman and Newman 1971) with the new confined compressive strength in the main axis being

$$f_{ck,c} = f_{ck}(1 + K) \tag{3.2b}$$

$$K \approx 3.7\left(\frac{p}{f_{ck}}\right)^{0.86} \tag{3.5}$$

Where $p(= \sigma_2 = \sigma_3)$ is uniform confining pressure at right angles to the nominal compressive stress, σ_1.

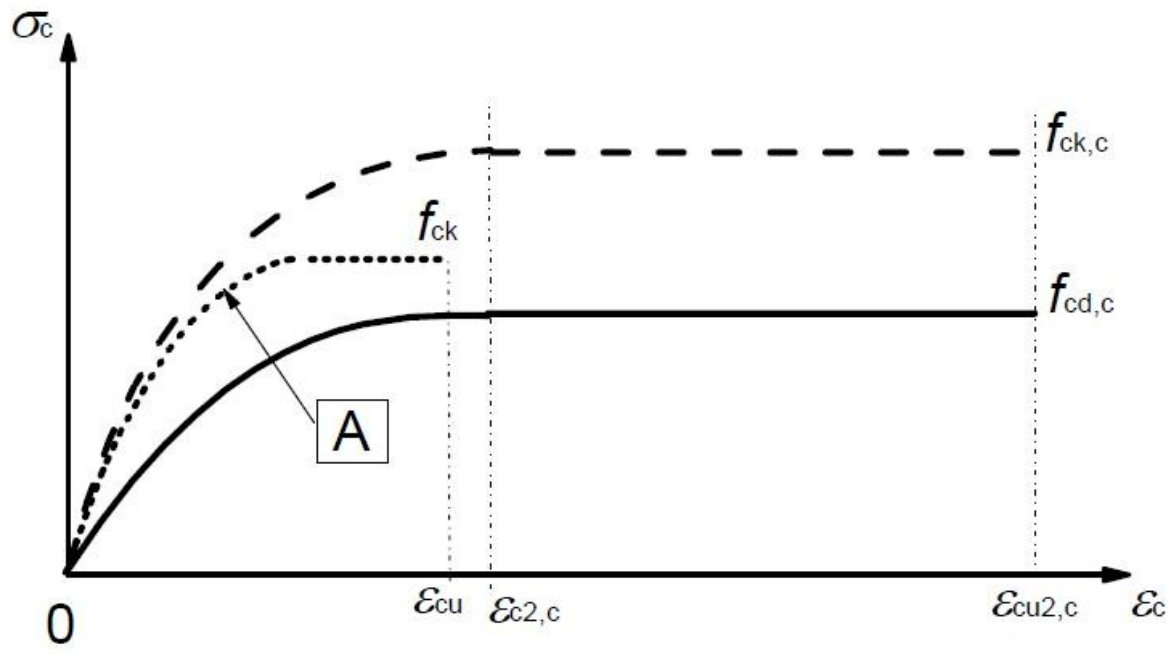

Figure 3-1: Stress-Strain Relation of Confined and Unconfined Concrete

According to Richart et al (1928) the following expression applies (adopted also in Eurocode 8 Part 3 (CEN 2005a)):

$$\varepsilon_{co,c} \approx \varepsilon_{co}(1 + 5K) \tag{3.3b}$$

Where $\varepsilon_{co,c}$ and ε_{co} compressive strain of confined and unconfined concrete at the peak stress.

Part 3 of Eurocode 8 (CEN 2005a) proposes the following for the ultimate strain at the extreme fibres of the confined concrete core in members under cyclic bending:

$$\varepsilon_{cu,c} = 0.004 + 0.5\frac{p}{f_{ck,c}} \qquad (3.4b)$$

Where $\varepsilon_{cu,c}$ is ultimate compressive strain of confined concrete core.

Note that even though the pair of equations for $Eqs\ (3.1), (3.2)$ and (3.3), noted as $a\ or\ b$ for their respective equations, have different expirations stand for the same material property of concrete. For example; $Eq(3.2b)$ gives a much higher value for strain at maximum strength than $(3.2a)$. Thus, the model for confinement given in ES-EN 1992:2015 will underestimate the enhancement by confinement as compared to ES-EN 1998:2015-3.

For a rectangular section, let b_{xo} and b_{yo} be the centerline dimensions of the ties. The minimum confined cross-sectional area mid-way between consecutive ties with area equal to the following fraction of the cross-section area inside the tie centerline:

$$a_s = \left(1 - \frac{s}{2b_{xo}}\right)\left(1 - \frac{s}{2b_{yo}}\right) \qquad (3.6)$$

with s being the spacing of ties and a_s notifying the coefficients of confinement effectiveness along the member.

At the level of a rectangular stirrup, the confined part of the cross-section is equal to the following fraction of the area enclosed by the centerline of the stirrup:

$$a_n = 1 - \frac{\sum {b_i}^2/6}{b_{xo}b_{yo}} \qquad (3.7)$$

Where b_i is the length of chords along the perimeter, and a_n notifies the coefficients of confinement effectiveness over the cross-section.

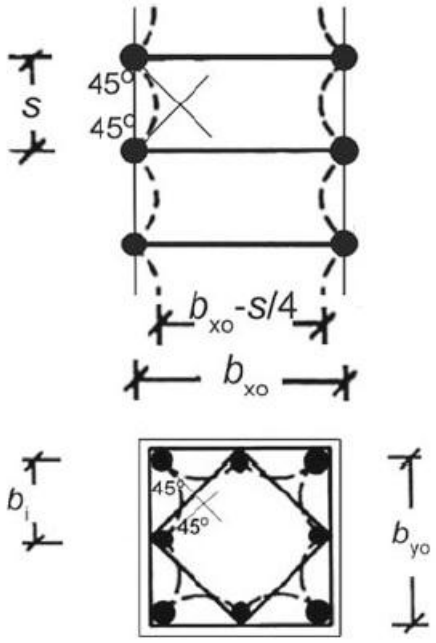

Figure 3-2: Confined and unconfined part over the cross-section along a member with square section and multiple ties

Factors a_s and a_n may be considered as coefficients of confinement effectiveness along the member, or over the cross-section, respectively. The combined confinement effectiveness factor is the product:

$$a = a_n a_s \tag{3.8}$$

A tensile stress $\sigma_s = f_{yw}$ in all stirrup legs and cross-ties parallel to transverse direction that opposes the dilatation of a concrete that approaches its ultimate strength, produces an average compressive stress p in the concrete, computed from equilibrium as:

$$\sigma_2/f_{ck} = p/f_{ck} = 0.5a\rho_w f_{yw}/f_{ck} = 0.5a\omega_w \tag{3.9}$$

Where: ω_w is the mechanical volumetric ratio of confining reinforcement: $\omega_w = \rho_w f_{yw}/f_c$, and ρ_w is the volumetric ratio of confining reinforcement and for transverse reinforcement having a spacing of s, is given by

$$\rho_w = 2\,min(\rho_x, \rho_y) = 2\,min\left(\sum A_{swx}/b_{yo}\,, \sum A_{swy}/b_{xo}\right)/s \tag{3.10}$$

Where: ρ_x and ρ_y are the fictitious volumetric ratio of confining reinforcement along x and y,

A_{swx} and A_{swy} are the total stirrup cross-section area parallel to transverse direction x and y respectively,

b_{xo} and b_{yo} are the centerline dimensions of the ties along transverse direction x and y respectively,

s is the spacing of transverse reinforcement.

3.1.2. Numerical Models for Reinforcement Steel

The stress-strain behavior used will be the simplified bilinear curve. The $\sigma - \varepsilon$ law of reinforcing steel is elastic-perfectly plastic at relatively low strains up to yielding plateau when $\varepsilon_s = \varepsilon_y$. As the strain is increased from ε_y, the steel is considered to strain-harden at the yield stress f_{yk}. Strain-hardening is linear, starting from the yield stress f_{yk} at a strain ε_{sh}, till the ultimate strength f_{tk} of steel at an elongation of ε_{su}. The $\sigma - \varepsilon$ parameters ($f_{yk}, \varepsilon_y = f_{yk}/E_s\,, \varepsilon_{sh}, f_{tk}, \varepsilon_{su}$) of tension, compression and web reinforcement are indexed by $1{,}2\ or\ v$, respectively.

$f_s = E_s\varepsilon_s \rightarrow$ up to yielding $\rightarrow -\varepsilon_{yd} \leq \varepsilon_s \leq \varepsilon_{yd}$

After yielding

For tension: $f_s = f_{yk}\left[1 + \left(f_{tk}/f_{yk} - 1\right)\left(\varepsilon_s - \varepsilon_{yd}\right)/\left(\varepsilon_{uk} - \varepsilon_{yd}\right)\right] \rightarrow \varepsilon_{yd} \leq \varepsilon_s \leq \varepsilon_{uk}$

For compression: $f_s = -f_{yk}\left[1 + \left(f_{tk}/f_{yk} - 1\right)\left(\varepsilon_s - \varepsilon_{yd}\right)/\left(\varepsilon_{uk} - \varepsilon_{yd}\right)\right] \rightarrow \varepsilon_{yd} \leq \varepsilon_s \leq \varepsilon_{uk}$

Where: f_s and ε_s are the compressive stress and strain on the reinforcing steel

f_{yk} and f_{tk} are the characteristic yield and ultimate strength of reinforcement

ε_{yk} and ε_{uk} are the characteristic yield and ultimate strain of reinforcement

E_s is modulus of elasticity of reinforcement

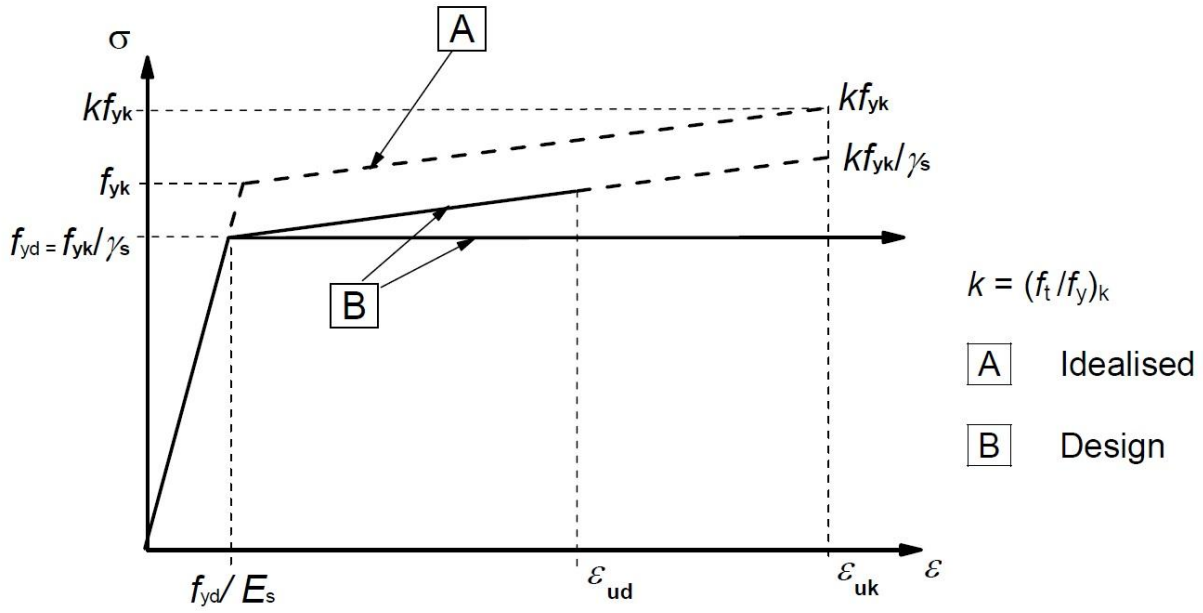

Figure 3-3: Stress-Strain Relation for Reinforcement Steel

3.2. Moment-Curvature ($M-\varphi$) Relation

3.2.1. Moment-Curvature ($M-\varphi$) Relation up to Yielding

For a cross-section with a rectangular compression zone, yielding of the whole section is identified if tensile reinforcement yields first or if concrete fibres located around the extremities of the section exceed a certain strain before yielding of tension steel. The latter of the two cases happens for a higher axial load ratio.

If the section yields when the tension steel yields first, the yielding curvature is given by

$$\varphi_y = \frac{f_{yL}}{E_s(1-\xi_y)d} \tag{3.11}$$

with φ_y is curvature at yield, f_{yL} being the yield stress of longitudinal bars, ξ_y the normalized neutral axis depth at yielding, and d is the effective depth of the cross-section.

$$\xi_y = (\alpha^2 A^2 + 2\alpha B)^{1/2} - \alpha A \tag{3.12}$$

$$\xi_y = \left(\alpha^2\left(\rho_1+\rho_2+\rho_v+\frac{N}{bdf_y}\right)^2+2\alpha\left(\rho_1+\rho_2\delta_1+0.5\rho_v(1+\delta_1)+\frac{N}{bdf_y}\right)\right)^{1/2}- \alpha\left(\rho_1+\rho_2+\rho_v+\frac{N}{bdf_y}\right) \quad (3.13)$$

Where $\alpha = E_s/E_c$; ρ_1 and ρ_2 are area reinforcement of tension and compression steel normalized to bd; ρ_v is the ratio of web reinforcements that are uniformly distributed between tension and compression steel; bd is the product of width and effective depth of the section; and $\delta_1 = d_1/d$ with d_1 being distance of the centre of the compression reinforcement from the extreme compression fibres.

However, if the section yields by concrete strain exceeding the limit of $\varepsilon_c \approx 1.8\, f_c/E_c$, which is mostly associated with high axial loads, the curvature at yielding will be

$$\varphi_y \approx \frac{1.8f_c}{E_c\xi_y d} \quad (3.14)$$

$$\xi_y = \left(\alpha^2\left(\rho_1+\rho_2+\rho_v+\frac{N}{\varepsilon_c E_s bd}\right)^2+2\alpha\left(\rho_1+\rho_2\delta_1+0.5\rho_v(1+\delta_1)\right)\right)^{1/2}-\alpha\left(\rho_1+\rho_2+\rho_v+\frac{N}{bdf_y}\right) \quad (3.15)$$

The lowest of the two φ_y given by $Eq(3.11)$ or $Eq(3.13)$ is the yielding curvature of the section. The yielding moment, M_y, calculated using equilibrium of forces on the section as

$$\frac{M_y}{bd^3} = \varphi_y\left\{E_c\frac{{\varphi_y}^2}{2}\left(\frac{1+\delta_1}{2}-\frac{\xi_y}{3}\right)+\frac{E_c(1-\delta_1)}{2}\left[\left(1-\xi_y\right)\rho_1+\left(\xi_y-\delta_1\right)\rho_2+\frac{\rho_v}{6}(1-\delta_1)\right]\right\} \quad (3.16)$$

Where M_y is the moment at yield and E_c is is modulus of elasticity of concrete.

3.2.2. Moment-Curvature ($M-\varphi$) Relation at Ultimate

3.2.2.1. Ultimate Curvature (φ)

A section is said to have reached its ultimate state under increasing deformation when either of the following two states is reached

1) If the tension reinforcement reaches its ultimate elongation, ε_{su}, and ruptures. This gives an ultimate curvature equal to:

$$\varphi_{su} = \frac{\varepsilon_{su}}{(1-\xi_{su})d} \tag{3.17}$$

Where φ_{su} is the ultimate curvature if steel ruptures first, ξ_{su} is the neutral axis depth (normalized to effective depth, d) when the ultimate curvature of the section is attained due to steel rupture, ε_{su} is strain of reinforcement at steel rupture.

2) Or if most of the compression zone disintegrates and sheds its compressive force. This takes place when the concrete of the extreme compression fibres reaches its ultimate strain, ε_{cu}, giving an ultimate curvature of:

$$\varphi_{cu} = \frac{\varepsilon_{cu}}{\xi_{cu}d} \tag{3.18}$$

Where φ_{cu} is the ultimate curvature if concrete reaches its ultimate strain, ε_{cu} first, ξ_{cu} is the neutral axis depth (normalized to effective depth, d) when the ultimate curvature for the same reason.

Depending on various parameters; such as level of axial load, amount and location of longitudinal bars and confinement level of compression zone, failure mode 1 or 2 can take place before or after spalling of the unconfined concrete cover.

3.2.2.2. Ultimate Moment Resistance

At these failure modes, confinement of core might be triggered depending on whether spalling of cover occurs or not. Therefore, to fully understand ultimate state, we need a further three distinct subcases under each mode.

For a sample cross-section under the action of axial load has three distinct ways it will fail.

a. Failure of full section due to rupture of tension reinforcement before spalling of concrete cover
b. Failure due to rupture of tension reinforcement after spalling of concrete cover

c. Failure of confined core after spalling of cover

The resistance capacity of the section is analysed using strain-stress relation and simple equilibrium of forces. For the first two cases of failures, the unconfined concrete properties are used. After the cover spalls and the stress along stirrups reach their yield strength value, confinement in the core will be triggered resulting in the use of enhanced strength and strain for the last case of failure. Further detailed discussion is presented in Annex A.

3.3. Curvature Ductility

Curvature ductility, which will be the main criteria for comparing the code in this paper, can be easily computed.

$$\mu_{\varphi} = \frac{\varphi_u}{\varphi_y} \tag{3.19}$$

With μ_{φ} being curvature ductility, φ_u is the ultimate curvature obtained from Section 3.2.2.1 and φ_y being the yield curvature from Section 3.2.2.2.

Figure 3-4 show a clear and useful flowchart for the steps followed of construct the new P-M interaction charts, along with the formulae for it.

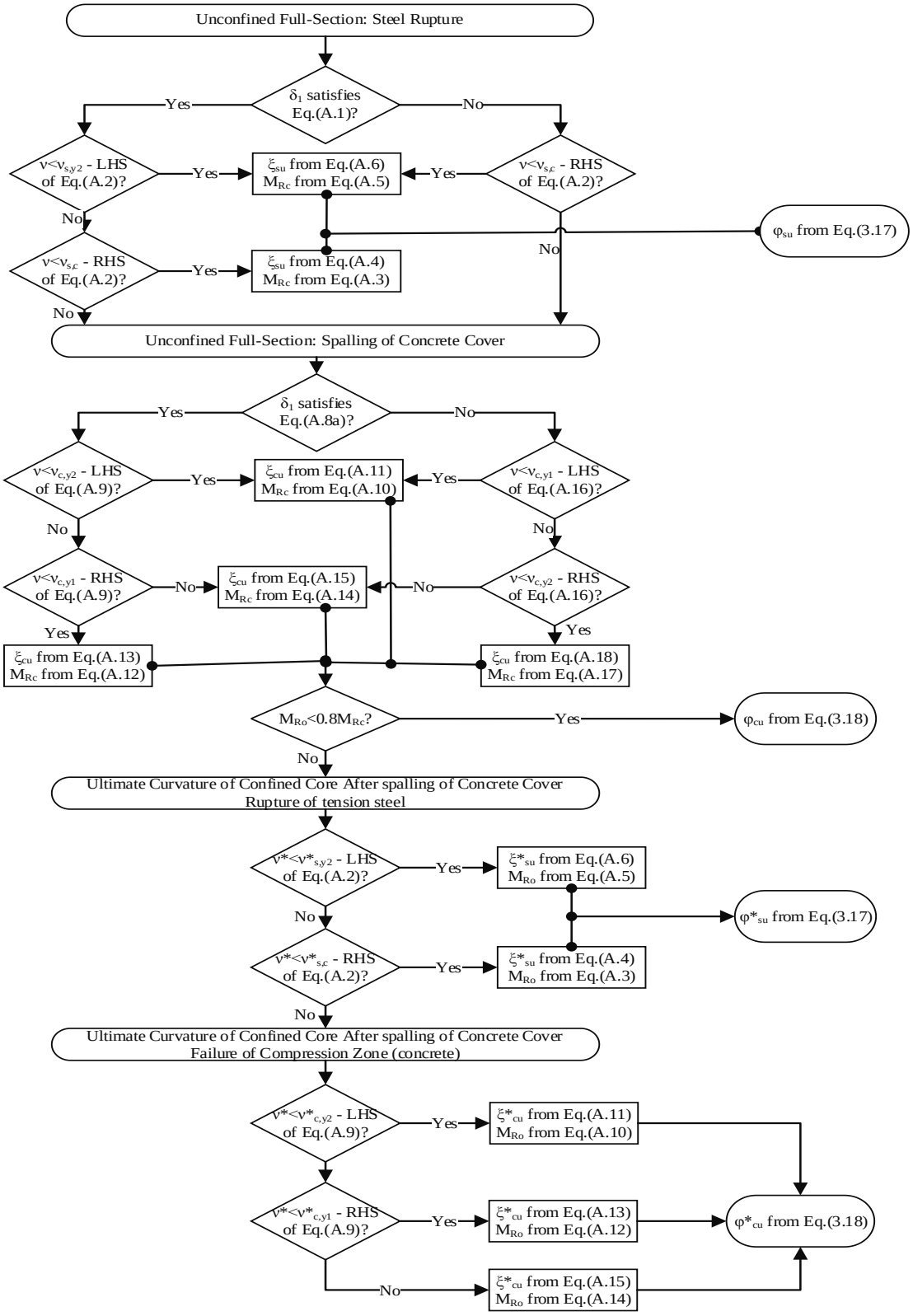

Figure 3-4: Flowchart for calculating interaction chart

CHAPTER 4: RESULTS AND DISCUSSIONS

4.1. Comparisons of Code Provisions

Although the definitions of the axial load ratio in the codes are not similar, they can be compared by changing the normalizing from the concrete design cylindrical strength to the characteristic cylindrical strength. The table below summaries the results.

Most of the codes studied in the paper stipulate some sorts of limits on the maximum value for design axial compressive loads. These limits are expressed in different form.

Some like ES EN 1998:2015, Eurocode 8, and GB 50011-2010 express their limits in terms of normalized axial loads; the design axial forces are normalized by the product of the gross concrete cross-sectional area and the design compressive strength of concrete, i.e., $A_c f_{cd}$. These three codes do not consider the strength coming for the longitudinal reinforcements. However, the Chinese code, require the limits need to be met even if the structure is not designed or checked for seismic activities, whilst the first two codes ignore their limits for low ductility classes.

Axial compression is limited by the nominal axial compressive strength of columns similar to non-seismic design, and it is dependent on the amount of longitudinal reinforcement for ACI, New Zealand, and Hong Kong codes.

It can be concluded that there is no consensus amongst different engineering and research communities on whether limiting the axial compression ratio is crucial to the ductile or capacity design of RC walls withstanding seismic loading [10]. In the era of globalization, there is a need for convergence of design methodologies to result in buildings with uniform risk of suffering a certain level of damage or collapse. A first step in this direction is to compare the expected seismic performance of buildings designed using the provisions of different codes.

Table 4-1: Comparison of code provisions

Codes	Expression of Limits	Are Longitudinal Reinforcement Considered?	Limits	Adjusted, v	Adjusted Limits
ES-EN1998:2015	$\frac{N_{Ed}}{A_c f_{cd}}$	NO	$\leq \begin{cases} - & \rightarrow DCL \\ 0.65 & \rightarrow DCM \\ 0.55 & \rightarrow DCH \end{cases}$	$\frac{N_{Ed}}{A_c f_{ck}}$	$\leq \begin{cases} - & \rightarrow DCL \\ 0.37 & \rightarrow DCM \\ 0.31 & \rightarrow DCH \end{cases}$
EC8	$\frac{N_{Ed}}{A_c f_{cd}}$	NO	$\leq \begin{cases} - & \rightarrow DCL \\ 0.65 & \rightarrow DCM \\ 0.55 & \rightarrow DCH \end{cases}$	$\frac{N_{Ed}}{A_c f_{ck}}$	$\leq \begin{cases} - & \rightarrow DCL \\ 0.43 & \rightarrow DCM \\ 0.37 & \rightarrow DCH \end{cases}$
ACI 318-14	$\frac{P_u}{P_o}$	YES	$\leq \begin{cases} 0.80 & \rightarrow Ties \\ 0.85 & \rightarrow Spirals \end{cases}$	$\frac{P_u}{A_c f_{ck}}$	$\leq \begin{cases} (0.68 + 0.8\omega - 0.68\rho) & \rightarrow Ties \\ (0.72 + 0.85\omega - 0.72\rho) & \rightarrow Spirals \end{cases}$
NZS 3101.1.206	$\frac{N_o^*}{N_{n,max}}$	YES	$\leq \begin{cases} 0.70 & \rightarrow Seismic \\ 0.85 & \rightarrow Non-Seismic \end{cases}$	$\frac{N_o^*}{A_c f_{ck}}$	$\leq \begin{cases} 0.60 + 0.7\omega - 0.60\rho \\ 0.72 + 0.85\omega - 0.72\rho \end{cases}$
GB 50011-2010	$\frac{N_{Ed}}{A_c f_c}$	NO	$\leq \begin{cases} 0.65 & \rightarrow Grade\ 1 \\ 0.75 & \rightarrow Grade\ 2 \\ 0.85 & \rightarrow Grade\ 3 \\ 0.90 & \rightarrow Grade\ 4 \end{cases}$	$\frac{N_{Ed}}{A_c f_{ck}}$	$\leq \begin{cases} 0.46 & \rightarrow Grade\ 1 \\ 0.54 & \rightarrow Grade\ 2 \\ 0.61 & \rightarrow Grade\ 3 \\ 0.64 & \rightarrow Grade\ 4 \end{cases}$
HKCode2013	N	YES	$\leq \begin{cases} 0.4 f_{cu} A_c + 0.75 A_{sc} f_y \\ 0.35 f_{cu} A_c + 0.67 A_{sc} f_y \end{cases}$	$\frac{N}{A_c f_{cd}}$	$\leq \begin{cases} 0.4 + 0.75\omega \\ 0.35 + 0.67\omega \end{cases}$

N.B: Hong Kong code does not have limiting value for normalized axial loads. Where $\omega = f_y A_{st} / A_c f_{ck}$ is the mechanical volumetric ratio, and $\rho = A_{st} / A_c$ is the ratio of reinforcement.

4.2. P-M Interaction Charts

A series of $\nu - \mu$ interaction charts for two parameters were plotted. The three main parameters studied are $\delta_1 = d_1/d$, mechanical reinforcement ratios $\omega = A_s f_y / A_c f_c$, and mechanical volumetric ratio of confining reinforcement ω_ω. The sections studied are strictly limited to symmetrical reinforced with respect to both sectional axis's, i.e., $A_{s1} = A_{s2} = A_s/4 \Longrightarrow \omega_1 = \omega_2 = \omega/4$ and $A_{sv} = A_s/2 \Longrightarrow \omega_v = \omega/2$; were the subscript $1, 2$ and v notify the tensile, compressive and web reinforcements, respectively. Since the value and shape of $\nu - \mu$ interaction charts are highly sensitive to values of ω_ω, the minimum recommended values of ω_ω as per ES-EN 1998:2015 for the two ductility classes, i.e. DCM and DCH. Therefore, two sets of values are considered for ω_ω.

Before proceeding, it is very crucial to differentiate the interaction chart presented in this paper from the design interaction charts. The first difference is the maximum material stress used. For design interaction chart the stresses used for concrete and reinforcements are design concrete compressive strength, $f_{cd} = \alpha_{cc} f_{ck}/\gamma_c$, and design yield strength, $f_{yd} = f_{yk}/\gamma_s$, respectively. However, the characteristic compressive cylinder strength of concrete, f_{ck}; and both the characteristic yield strength of reinforcement, f_{yk}, characteristic ultimate strength of reinforcement, f_{tk}, are used for this study.

The second difference, is the consideration of confinement effect due to transverse reinforcement. After ultimate compressive strain in the extreme fiber concrete in compression is reached, confined concrete properties stated in Section 3.1.1.2 will be utilised.

The limits on axial compressive loads by the code is expressed in terms of ratio of bhf_{cd}. Therefore, the ultimate axial loads are normalised by bhf_{cd}, while the ultimate moments are normalised by $bh^2 f_{cd}$. This will be helpful when comparing the results obtained to the limits.

All the chart calculated are presented in Annex B.

4.3. Normalised Balanced Axial Load

There is no clear-cut effect of the column's flexural behaviour if the value of axial force varies around the column balanced load [1]. However, it will be safe to say high axial compression, especially above the balanced load, highly influences the moment-curvature behavior and failure modes.

Therefore, the basic reason for limiting compressive axial loads on seismic resisting columns is to avoid brittle failure. Eurocode goes about this by limiting the normalized design axial compressive load, v, to 0.65 & 0.55 for Medium and High Ductility class respectively. These numbers were selected not because of any specific experiments, but rather are related to axial forces at balanced failure.

The limits set on normalized axial for both ductility classes are to ensure axial loads are very near to the balanced load point [17]. We can see from any $P-M$ interaction charts that, generally speaking, balanced failure occurs on normalized axial load, $v = P/A_c f_{ck}$, ranging from 0.43 to 0.37 depending on the value of δ_1.

For example, here is how the limit for DCM was derived. Let us take the upper bound value of, $v = 0.43$. For the load to be less than the balanced value the following inequality must be true.

$$v = \frac{N_{Ed}}{A_c f_{ck}} \leq 0.43 \tag{4.1}$$

where; v is the normalised axial load, N_{Ed} is the design axial force, A_c is the cross-sectional area of the column and f_{ck} is the characteristic cylindrical strength of concrete.

According to EN 1992:2015 Part 1-1 3.1.6(1), the design strength of concrete, f_{cd}, given as

$$f_{cd} = \alpha_{cc} f_{ck}/\gamma_c \tag{4.2}$$

where: α_{cc} and γ_c are safety factors accounting for loading type and long-term effects, and have values of 1.0 and 1.5 respectively. Therefore, $f_{cd} = f_{ck}/1.5 \rightarrow f_{ck} = 1.5 f_{cd}$, inserting this in the equation for v we can get v_d

$$v = \frac{N_{Ed}}{1.5 A_c f_{cd}} = \frac{v_d}{1.5} \leq 0.43 \rightarrow v_d \leq 0.65 \quad (4.3)$$

Where, $v_d = N_{Ed}/A_c f_{cd}$ is the axial load normalised to the design compressive strength of the concrete section.

On the other hand, the limiting value for DCH of $v_d = 0.55$ can be derived by taking $v \cong 0.37$, which is the lower bound. Using the same pervious logic, for DCM, for Eurocode

$$v = \frac{v_d}{1.5} \leq 0.37 \rightarrow v_d \leq 0.55 \quad (4.4)$$

However, according to ES-EN 1992:2015 part 1-1 3.1.6(1), the recommended value of the coefficient for long-term effects on the compressive strength of concrete $\alpha_{cc} = 0.85$. so for our code the only difference will be $0.85 f_{cd}$ instead of f_{cd}.

For DCM:

$$v_d = \frac{N_{Ed}}{0.85 A_c f_{cd}} = 0.65 \rightarrow v_{d,DCM} \leq 0.55 \quad (4.5)$$

For DCH:

$$v_d = \frac{N_{Ed}}{0.85 A_c f_{cd}} = 0.55 \rightarrow v_{d,DCH} \leq 0.47 \quad (4.6)$$

The above equations suggest we are currently designing column as DCH instead of DCM, as compared to Eurocode, because of the difference in the value of α_{cc}. This parameter is left for future investigation and will not be explored future in this paper.

Using the procedure outlined in Annex A, the ultimate moment resistance capacities, μ_u, ultimate curvature φ_u, curvature at yield, φ_y, and finally the curvature ductility, μ_φ, for the same values of δ_1 and ω. The same was done for axial load ratio having values of $v_d = 0.65$ and 0.55, normalised by $f_{cd} = 0.85\, f_{ck}/1.5$ as per ES-EN 1992:2015 recommendations. Then these results were compared with their respective balanced failure points to see the effects.

Fig 4 and 5 isolates and clearly shows where the balanced failure points on the chart, in relation to the limits are located, i.e., the $\nu_{u,Bal}$, for different values of δ_1.

- **For DCM**

The minimum specified design mechanical volumetric ratio of confining hoops within the critical regions at the base of primary seismic columns, $\omega_{\omega d}$, for DCM is 0.08. ES-EN1998:2015-8-1 §5.4.3.4.2(9) defines $\omega_{\omega d}$ as

$$\omega_{\omega d} = \frac{volume\ of\ confining\ hoops}{volume\ of\ concrete\ core}\frac{f_{yd}}{f_{cd}} \geq 0.08 \qquad (4.7a)$$

However, for this study ω_ω is expressed in terms of ratio of characteristic strength for both reinforcement and concrete, i.e., f_{yk}/f_{ck}. Adjusting for these factors, ω_ω will be

$$\omega_\omega = \frac{\alpha_{cc}*\gamma_s}{\gamma_c}\omega_{\omega d} \rightarrow \frac{0.85*1.15}{1.5}0.08 \rightarrow \omega_\omega = 0.052 \qquad (4.7b)$$

Fig. 4.1 shows for $\delta_1 = 0.05, 0.10, \text{and } 0.15$, the balanced failure point occurs at a normalised axial load of much higher than $\nu = 0.65$. However, for $\delta_1 = 0.20, \text{and } 0.25$ the $\nu_{bal} < 0.65$.

For $\delta_1 = 0.05$, the balanced failure point occurs at a normalised axial load of much higher than $\nu = 0.65$. it has an average value of $\nu_{bal} = 0.88$, (maximum value being $\nu_{bal} = 0.91$ for $\omega = 0.1$ and gradually decreasing to its minimum value of $\nu_{bal} = 0.86$ for $\omega = 2.0$). The decrease of ν_{bal} with an increase mechanical volumetric ratio ω, is consistent with our well-known knowledge that suggest the likelihood for ductile failure occurring at a lower action threshold for a section with higher reinforcement than a lightly reinforced section.

For $\delta_1 = 0.10, \text{and } 0.15$, the mean normalised axial load at which balanced failure ensue at $\nu_{bal} = 0.79$ (ranging from 0.81 for $\omega = 0.1$ to 0.76 for $\omega = 2.0$), and $\nu_{bal} = 0.70$ (ranges from 0.73 for $\omega = 0.1$ to 0.68 for $\omega = 2.0$), respectively.

Balanced failures occur around $\nu_{bal} = 0.63$ (ranges from 0.66 for $\omega = 0.1$ to 0.61 for $\omega = 2.0$), and $\nu_{bal} = 0.57$ (ranges from 0.59 for $\omega = 0.1$ to 0.54 for $\omega = 2.0$) for $\delta_1 = 0.20, \text{and } 0.25$, respectively.

- **For DCH**

The minimum value of $\omega_{\omega d}$ to be provided in subclause 10 of ES-EN1998:2015-8-1 §5.5.3.2.2 is 0.12 within the critical region atthe base of the column, or 0.08 in all column critical regions above the base.

$$\omega_{\omega} = \frac{\alpha_{cc} * \gamma_s}{\gamma_c} \omega_{\omega d} \rightarrow \frac{0.85 * 1.15}{1.5} 0.12 \rightarrow \omega_{\omega} = 0.0782 \quad (4.8)$$

It can be observed from Fig. 4.2 that balanced failure point occurs at a normalised axial load of greater than $v = 0.55$ for all values of δ_1 considered.

Balanced failures occur around $v_{bal} = 0.91$ (ranging from a maximum value of 0.93 for $\omega = 0.1$ to a minimum of 0.90 for $\omega = 2.0$), $v_{bal} = 0.82$ (ranges from 0.83 for $\omega = 0.1$ to 0.80 for $\omega = 2.0$), $v_{bal} = 0.73$ (from 0.75 for $\omega = 0.1$ to 0.72 for $\omega = 2.0$), $v_{bal} = 0.66$ (its value ranging $0.67 - 0.64$), $v_{bal} = 0.59$ (with it value being 0.61 for $\omega = 0.1$ to 0.58 for $\omega = 2.0$). the aforementioned values of v_{bal} are for $\delta_1 = \ 0.05, 0.10, 0.15, 0.20, \text{and } 0.25$ respectively.

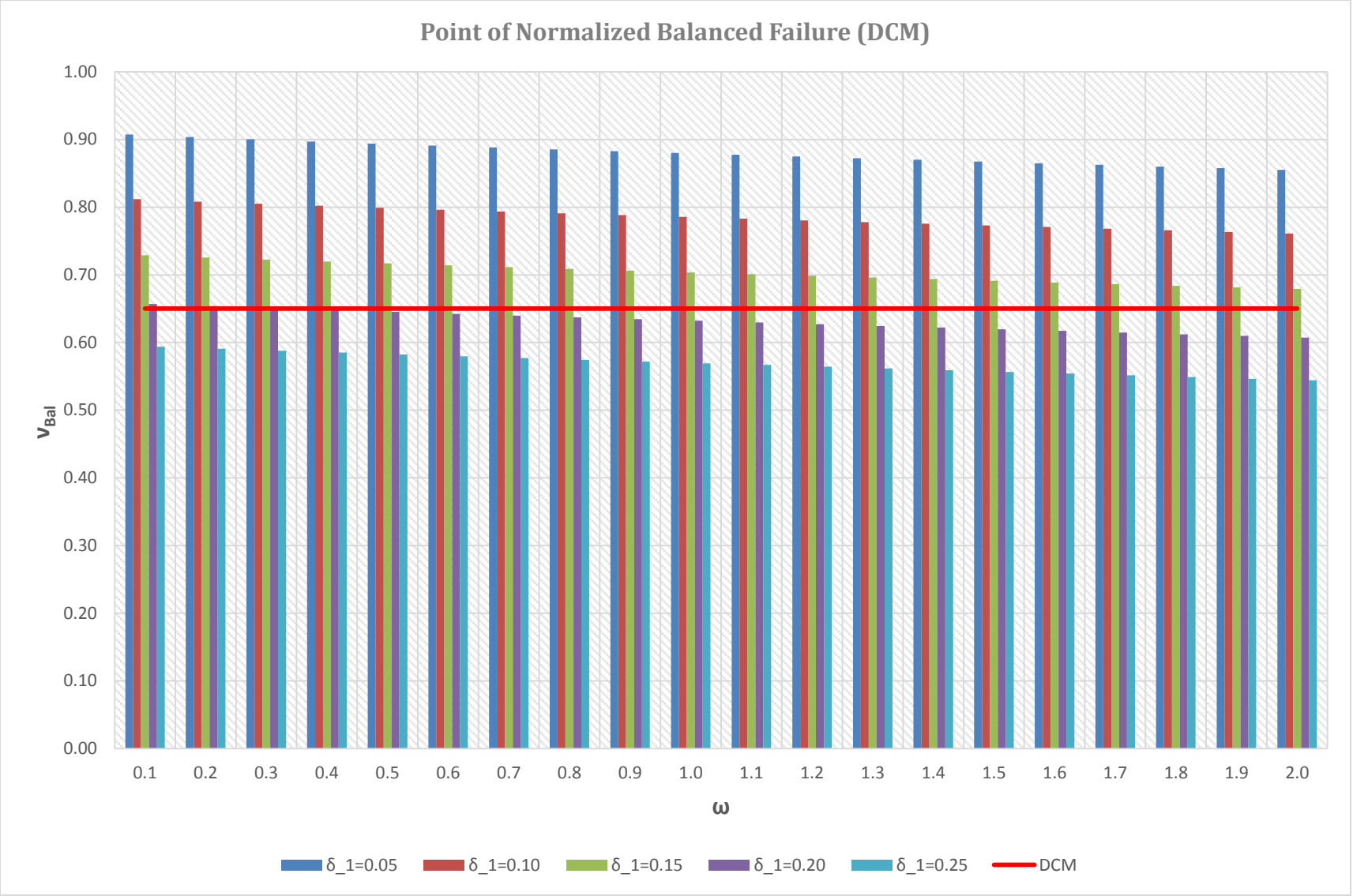

Figure 4-1: Normalized Balanced Axial Loads (DCM)

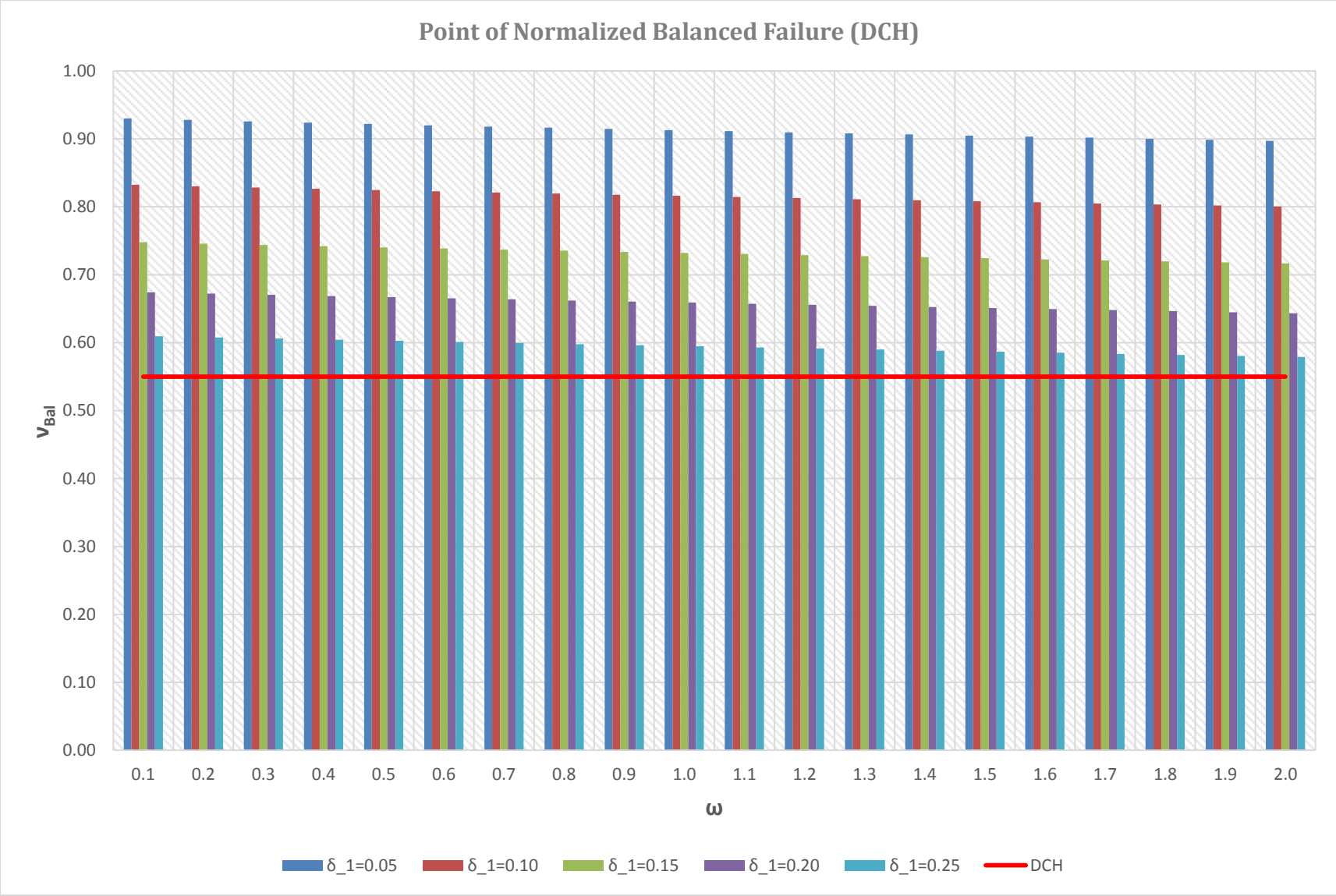

Figure 4-2: Normalized Balanced Axial Loads (DCH)

4.4. Curvature at Yielding, Ultimate Curvature and Curvature Ductility

The power of curvature ductility, μ_φ, in assessing the ductile behaviour of a reinforced concrete is immense. It is considered as an appropriate indicator of the adequacy of earthquake resistant design for reinforced concrete members. This power is utilized in this paper to check the state of ductility under the calculated balanced loads and compare it with ones under code provisions.

The ductility capacity of reinforced concrete sections is usually expressed in terms of the curvature ductility ratio given by $Eq.(3.19)$. Before we proceed to comparing the curvature ductility, lets us first compare curvature at yielding, φ_y, and ultimate curvature, φ_u,.

- **Comparisons with DCM**

The comparison is made by comparing the ratio of curvature at yielding, $\varphi_{y,DCM}$, and ultimate curvature, $\varphi_{u,DCM}$, with values $\varphi_{y,Bal}$ and $\varphi_{u,Bal}$ respectively.

N.B: Both $\varphi_{y,DCM}$ and $\varphi_{u,DCM}$ are calculated at $\nu = 0.65$, while $\varphi_{y,Bal}$ and $\varphi_{u,Bal}$ are curvatures at yielding and ultimate for the calculated v_{bal}. The rate gain or loss for each parameter will be calculated as Eq 4.9. The same logic is followed for rate of change in ultimate curvature, $\Delta_{\varphi,u,DCM}$, and rate of change in curvature ductility, $\Delta_{\mu,\varphi,DCM}$.

$$\Delta_{\varphi,y,DCM} = \left(\frac{\varphi_{y,Bal} - \varphi_{y,DCM}}{\varphi_{y,DCM}}\right) * 100 \tag{4.9}$$

Where: $\Delta_{\varphi,y,DCM}$ is the percentage change in curvature at yield, $\varphi_{y,Bal}$ and $\varphi_{y,DCM}$ are the curvature at yield for ν values of ν_{Bal} and 0.65, respectively.

The comparison of curvatures at both yield and ultimate state at balanced failure with limits set to fulfil conditions of DCM are presented here within.

It can be seen in Table 4.2, that the curvature at yielding increases by an average of 5.6%, 3.4%, and 1.4% for $\delta_1 = 0.05, 0.10$, and 0.15 respectively. While φ_y decreases by a mean of 0.4%, and 2.1% for $\delta_1 = 0.20$, and 0.25 respectively.

Contrary to curvature at yielding, ultimate curvature shows a decrease for values of $\delta_1 = 0.05, 0.10$, and 0.15, with its average respective decrease of 14.0%, 8.8%, and 3.8%. For $\delta_1 = 0.20$, and 0.25, the respective mean gain in φ_u increases by an average of 0.9%, and 5.3%.

The change in curvature ductility follows the same trend as that of ultimate curvature for the same values of δ_1. μ_φ decreases by an average of 18.4%, 11.8%, and 5.2% for $\delta_1 = 0.05, 0.10$, and 0.15, while having the mean gain of 1.3%, and 7.6% for $\delta_1 = 0.20$, and 0.25, respectively.

Table 4-2: Summary of average and change in values of parameters (DCM)

Parameters		δ_1				
		0.05	**0.10**	**0.15**	**0.20**	**0.25**
Average: Chart	$\mu_{u,Bal}$	0.7943	0.6719	0.5699	0.4842	0.4117
	$\nu_{u,Bal}$	0.8796	0.7850	0.7029	0.6313	0.5683
	$\varphi_{u,Bal}$	0.0142	0.0147	0.0152	0.0157	0.0163
	$\varphi_{y,Bal}$	0.0039	0.0039	0.0040	0.0040	0.0040
	$\mu_{\varphi,Bal}$	3.6015	3.7140	3.8248	3.9336	4.0403
Average: DCM	$\mu_{u,DCM}$	0.7869	0.6694	0.5695	0.4842	0.4111
	ν_{DCM}	0.6500	0.6500	0.6500	0.6500	0.6500
	$\varphi_{u,DCM}$	0.0165	0.0161	0.0158	0.0156	0.0154
	$\varphi_{y,DCM}$	0.0037	0.0038	0.0039	0.0040	0.0041
	$\mu_{\varphi,DCM}$	4.4395	4.2233	4.0396	3.8842	3.7536
Change (%)	$\Delta_{\mu,u,Ave,DCM}$	1.5%	0.6%	0.1%	0.0%	0.2%
	$\Delta_{Ave,\varphi y,DCM}$	5.6%	3.4%	1.4%	-0.4%	-2.1%
	$\Delta_{Ave,\varphi u,DCM}$	-14.0%	-8.8%	-3.8%	0.9%	5.3%
	$\Delta_{Ave,\mu\varphi,DCM}$	-18.4%	-11.8%	-5.2%	1.3%	7.6%

- **Comparisons with DCH**

The comparison is the same for that of DCM, with the exception being the parameters; $\varphi_{y,DCH}$ and $\varphi_{u,DCH}$ are calculated curvature at yielding and ultimate state, respectively, and $\mu_{\varphi,DCH}$ is the curvature ductility when $\nu = 0.55$.

The comparison results of curvatures at both yield and ultimate state at balanced failure with limits set to fulfil conditions of DCH are shown in Table 4.3.

There is a census increase in φ_y when compared to its respective $\varphi_{y,DCH}$ for all values of δ_1. Curvature at yielding increases by an average of 9.1%, 6.9%, 4.9%, 3.0%, and 1.3% for $\delta_1 = 0.05, 0.10, 0.15, 0.20$, and 0.25 respectively.

On the contrary, there appears to be a census decrease for both ultimate curvature and curvature ductility. The average respective decrease in φ_y for $\delta_1 = 0.05, 0.10, 0.15, 0.20$, and 0.25 is 21.4%, 16.6%, 12.0%, 7.5%, and 3.3%. Whereas, the mean loss in μ_φ is 27.8%, 21.8%, 16.0%, 10.2%, and 4.5% for the same respective values of δ_1.

Table 4-3: Summary of average and change in values of parameters (DCH)

Parameters		δ_1				
		0.05	**0.10**	**0.15**	**0.20**	**0.25**
Average: Chart	$\mu_{u,Bal}$	0.8016	0.6780	0.5749	0.4884	0.4153
	$\nu_{u,Bal}$	0.9127	0.8157	0.7317	0.6583	0.5940
	$\varphi_{u,Bal}$	0.0179	0.0185	0.0192	0.0199	0.0206
	$\varphi_{y,Bal}$	0.0040	0.0040	0.0040	0.0040	0.0041
	$\mu_{\varphi,Bal}$	4.5191	4.6629	4.8044	4.9434	5.0796
Average: DCH	$\mu_{u,DCH}$	0.7841	0.6690	0.5710	0.4871	0.4150
	ν_{DCH}	0.5500	0.5500	0.5500	0.5500	0.5500
	$\varphi_{u,DCH}$	0.0229	0.0223	0.0219	0.0215	0.0213
	$\varphi_{y,DCH}$	0.0036	0.0037	0.0038	0.0039	0.0040
	$\mu_{\varphi,DCH}$	6.3365	6.0228	5.7543	5.5253	5.3308
Change (%)	$\Delta_{\mu,u,Ave,DCH}$	3.4%	2.1%	1.1%	0.5%	0.1%
	$\Delta_{Ave,\varphi y,DCH}$	9.1%	6.9%	4.9%	3.0%	1.3%
	$\Delta_{Ave,\varphi u,DCH}$	-21.4%	-16.6%	-12.0%	-7.5%	-3.3%
	$\Delta_{Ave,\mu\varphi,DCH}$	-27.8%	-21.8%	-16.0%	-10.2%	-4.5%

4.5. Example Case Studies

For further illustration, fifteen sample column section having various geometric properties will be discussed here. The sections are classified under three distinct case group each with five different sections. The three parameters for categorising the sections are; normalised distance of compression reinforcement from the extreme compression fibres with respect to effective depth, δ_1, mechanical reinforcement ratios, ω, and the mechanical volumetric ratio of confining reinforcement, ω_ω.

The fifteen sections were selected to represent column cross-section that are commonly encountered in every day design. Their geometrical description is listed in Table 4.4, and their sectional details are shown in Fig. 4.3 below.

Table 4-4: List of sectional properties considered for case study

bxh	Section	Re-bar	Cover	$\phi_{Stirrup}$	Spacing (Stirrup)	δ_1	ω	ω_ω
300X300	1-A	4ϕ16	15	8	110	**0.12**	0.20	0.14
400X400	1-B	12ϕ16	35	8	100	**0.15**	0.20	0.14
500X500	1-C	24ϕ14	60	8	130	**0.18**	0.20	0.14
600X600	1-D	16ϕ16	35	10	170	**0.10**	0.20	0.14
800X800	1-E	24ϕ20	20	10	140	**0.05**	0.20	0.14
500X500	2-A	16ϕ14	30	8	100	0.10	0.20	**0.09**
600X600	2-B	20ϕ20	35	10	100	0.10	0.20	**0.19**
700X700	2-C	28ϕ16	45	10	100	0.10	0.20	**0.34**
800X800	2-D	24ϕ20	50	10	100	0.10	0.20	**0.21**
900X900	2-E	24ϕ20	60	12	120	0.10	0.20	**0.29**
500X500	3-A	16ϕ14	30	8	100	0.10	**0.17**	0.15
600X600	3-B	20ϕ20	35	10	130	0.10	**0.31**	0.15
700X700	3-C	28ϕ24	40	10	115	0.10	**0.45**	0.15
800X800	3-D	24ϕ20	50	10	150	0.10	**0.21**	0.15
900X900	3-E	36ϕ32	55	12	190	0.10	**0.63**	0.15

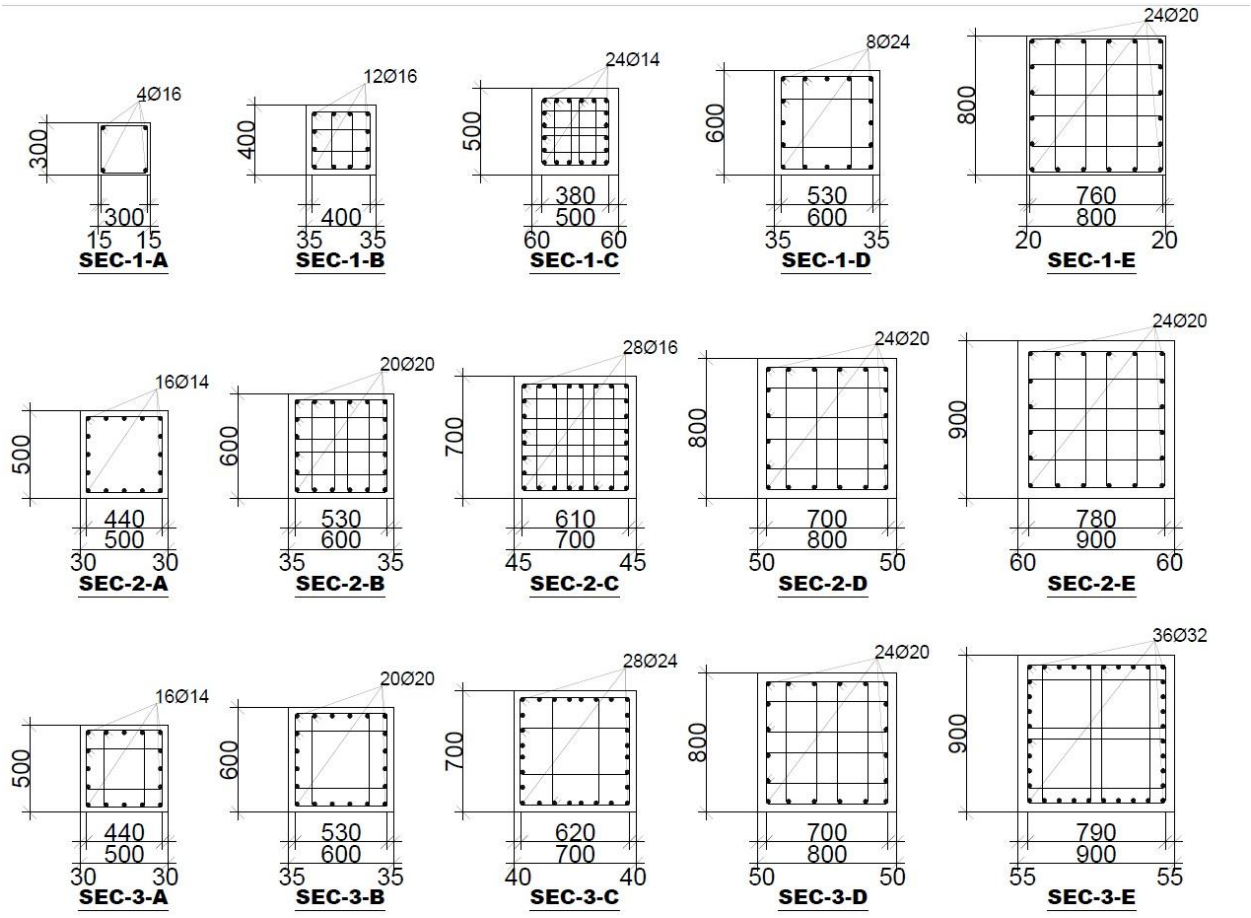

Figure 4-3: Column cross-sections considered for study

- **Case 1: Section 1-A to 1-E**

For the first case the varying parameter considered is δ_1, while both ω and ω_ω are kept relatively constant. All the resulting values are summarised in Table 4.5 with Fig 4.4 showing their $v - \mu$ interaction charts. The value of δ_1 selected ranges from 0.05 for 1-E to 0.18 for 1-C, and their respective value of v_{bal} are 0.9482 and 0.5793 (see Fig. 4.5). For the considered samples, the resulting mean v_{bal} is 0.7447 with a coefficient of variation of 16.5%. It can be reasonable to deduce, similar to results of the Section 4.3 shown in Annex B (Fig B.1 to B.10), that v_{bal} is highly sensitive the values of δ_1. The relationship between v_{bal} and δ_1 is inversely proportional, i.e., v_{bal} decreasing when δ_1 increases. Ultimate moment resistance of the sections at balanced failure, $\mu_{u,bal}$, flows the same trend as v_{bal}, decreasing with increasing δ_1. It has a mean value of 0.2479 with a coefficient of variation of 20.0%. Since all the other parameter, φ_y, φ_u, and μ_φ,

as shown in Table 4.5 below are all highly dependent on values of v_{bal}, they too are dependent on δ_1.

It is worth mentioning the anomaly of the results for Section 1-A. This is due to the lack of web reinforcement. Owing to the use of only four corner reinforcement, its curvature ductility, μ_φ, is lower when compared to the other sections in this set of case. This statement is further echoed by the requirement of at least one intermediate bar between corner bars along each column side as stipulated by ES EN 1998:2015 for both DCM and DCH. The provision of these intermediate bars is also necessary to ensure the integrity of beam-column joints.

Table 4-5: Results of Case - 1

Section	1-A	1-B	1-C	1-D	1-E	Average	Coefficient of Variation
$\mu_{u,Bal}$	0.2481	0.2150	0.1828	0.2632	0.3301	**0.2479**	**20.0%**
$\nu_{u,Bal}$	0.7402	0.6708	0.5793	0.7849	0.9482	**0.7447**	**16.5%**
$\varphi_{u,Bal}$	5.37E-05	7.04E-05	6.24E-05	4.20E-05	3.53E-05	**5.28E-05**	**24.4%**
$\varphi_{y,Bal}$	1.31E-05	1.16E-05	9.97E-06	6.50E-06	5.15E-06	**9.27E-06**	**32.5%**
$\mu_{\varphi,Bal}$	4.0939	6.0594	6.2599	6.4640	6.8613	**5.9477**	**16.2%**

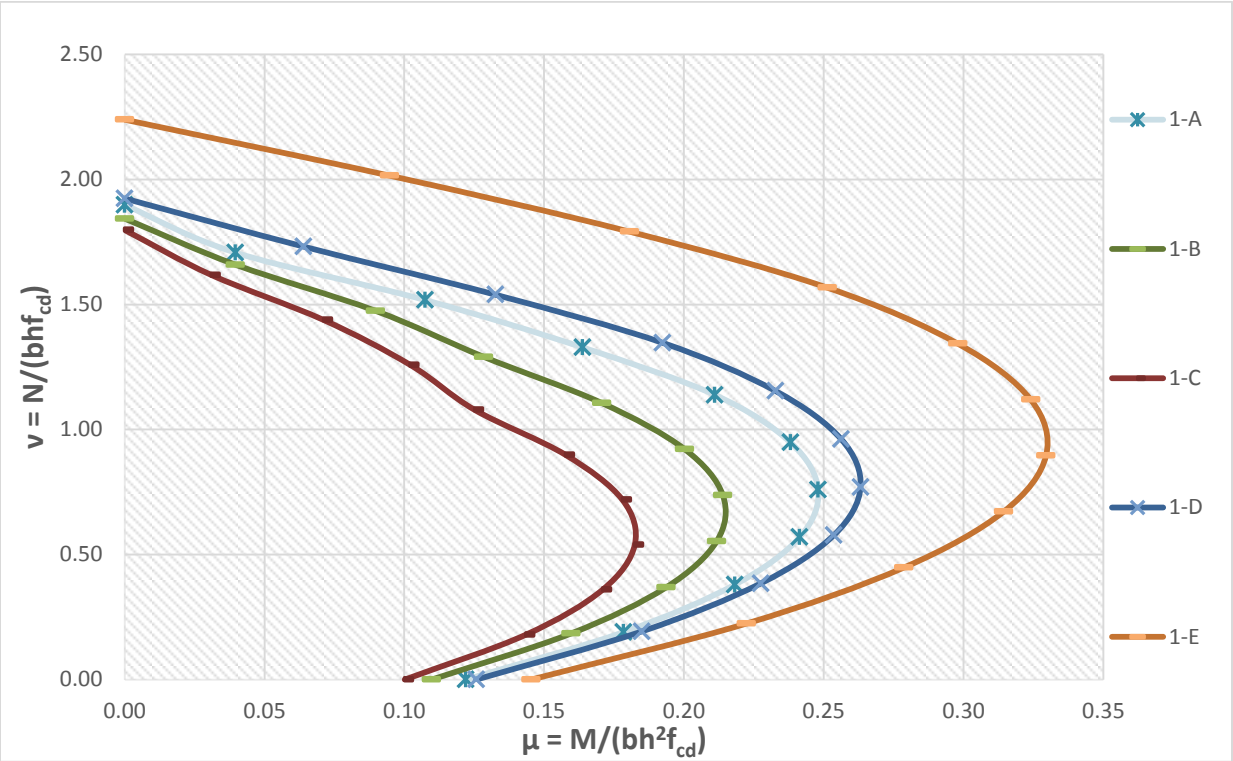

Figure 4-4: ν-μ Interaction for Case -1

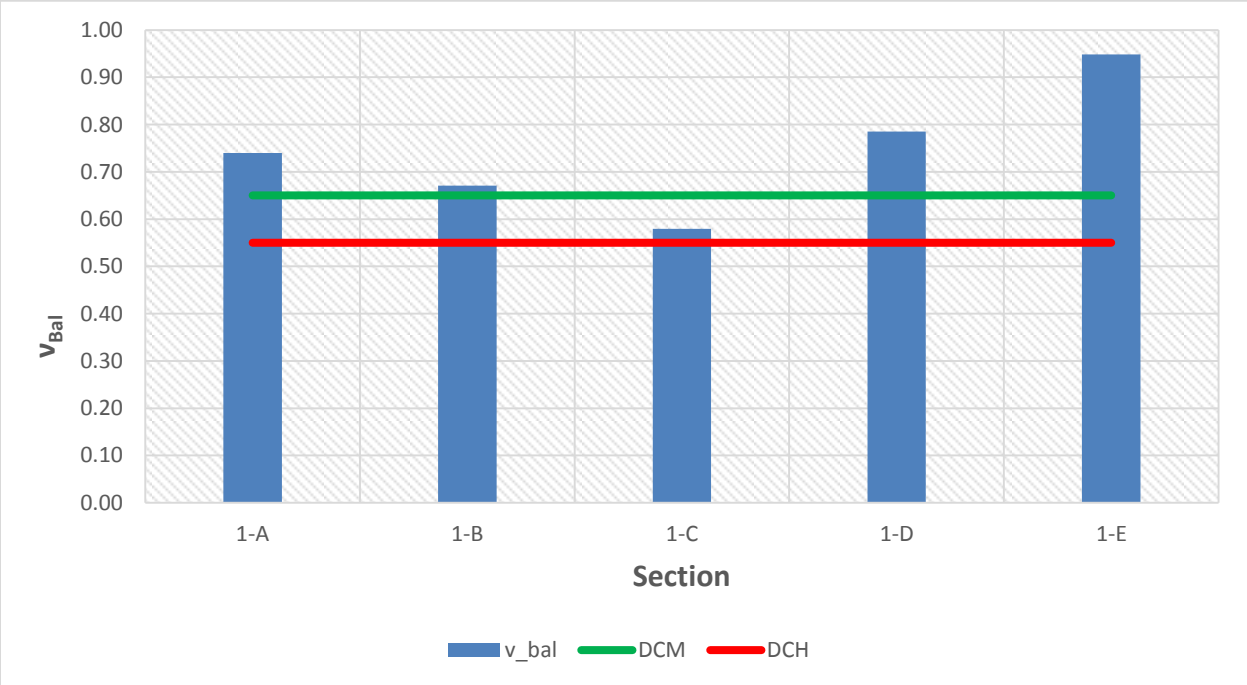

Figure 4-5: Normalised Balanced Load for Case -1

- **Case 2: Section 2-A to 2-E**

For the second case, ω_ω is varied while both ω and δ_1 are kept relatively constant. Fig. 4.5 shows the $v-\mu$ interaction charts and Table 4.6 presents a summary of results for case - 2. For these five set of sections, ω_ω varies from a minimum of 0.09 for section 2-A to a maximum of 0.34 for 2-C. Their corresponding v_{bal}, as illustrated in Fig. 4.7, are 0.7236 and 0.9156. The resulting average of v_{bal} is 0.8389 with its coefficient of variation of 7.7%. The output obtained imply that v_{bal} increases with increasing ω_ω. However, the influence of ω_ω on v_{bal} is relatively lower when compared to δ_1.

The values of $\mu_{u,bal}$, φ_y, φ_u, and μ_φ are enhanced by increasing ω_ω. Ultimate moment at balanced failure, $\mu_{u,bal}$, has a mean value of 0.2756 with a coefficient of variation of 4.9%. The results for the curvature properties are: φ_y averages at $6.37 * 10^{-6}\, rad/mm$ with coefficient of variation of 21.6%, the mean value of φ_u is $6.09 * 10^{-5}\, rad/mm$ with coefficient of variation of 36.2%, and finally curvature ductility has an average of 10.2609 with coefficient of variation of 42.2%.

The irregularity noticed on 2-A for values of φ_u and μ_φ, can be attributed to the absence of cross-tie or hoop confinements.

Table 4-6: Results of Case - 2

Section	2-A	2-B	2-C	2-D	2-E	Average	Coefficient of Variation
$\mu_{u,Bal}$	0.2513	0.2740	0.2917	0.2794	0.2816	**0.2756**	**4.9%**
$v_{u,Bal}$	0.7236	0.8312	0.9156	0.8489	0.8751	**0.8389**	**7.7%**
$\varphi_{u,Bal}$	2.64E-05	6.43E-05	9.53E-05	5.51E-05	6.36E-05	**6.09E-05**	**36.2%**
$\varphi_{y,Bal}$	7.83E-06	8.01E-06	6.19E-06	5.32E-06	4.49E-06	**6.37E-06**	**21.6%**
$\mu_{\varphi,Bal}$	3.3716	8.0276	15.4020	10.3596	14.1436	**10.2609**	**42.2%**

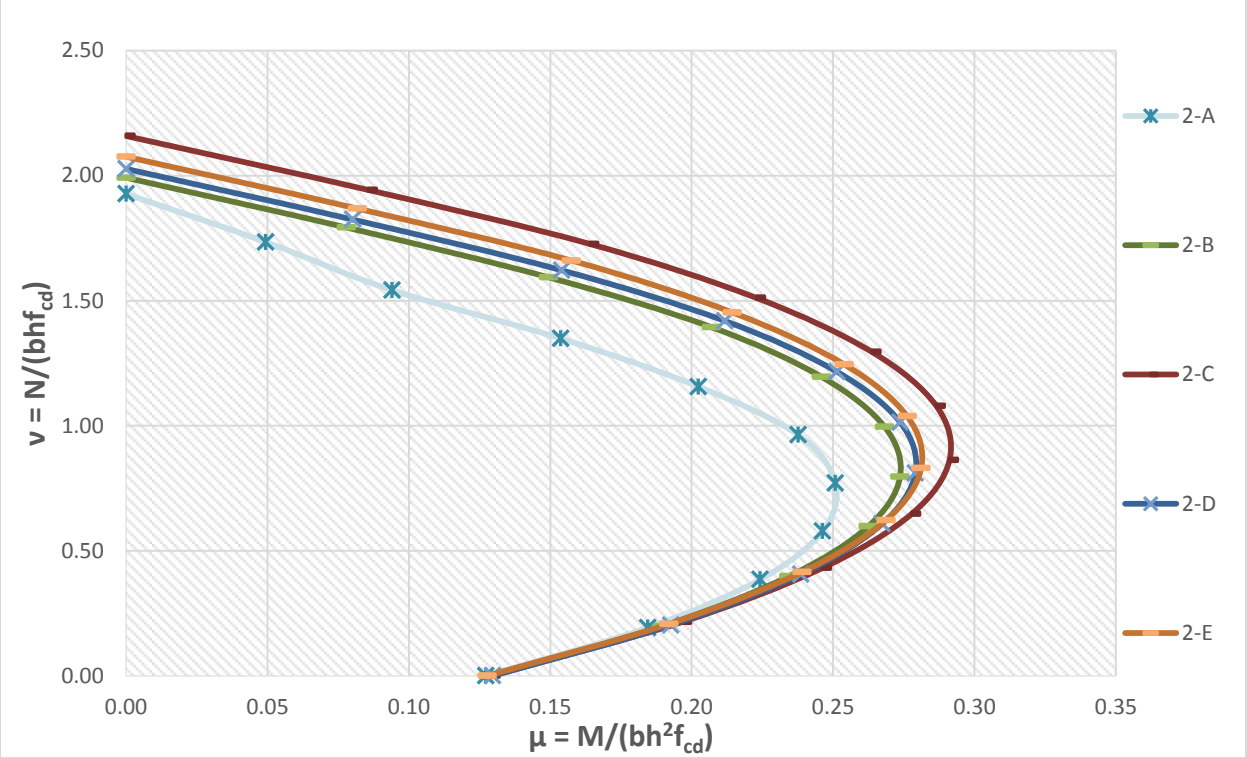

Figure 4-6: ν-μ Interaction for Case -2

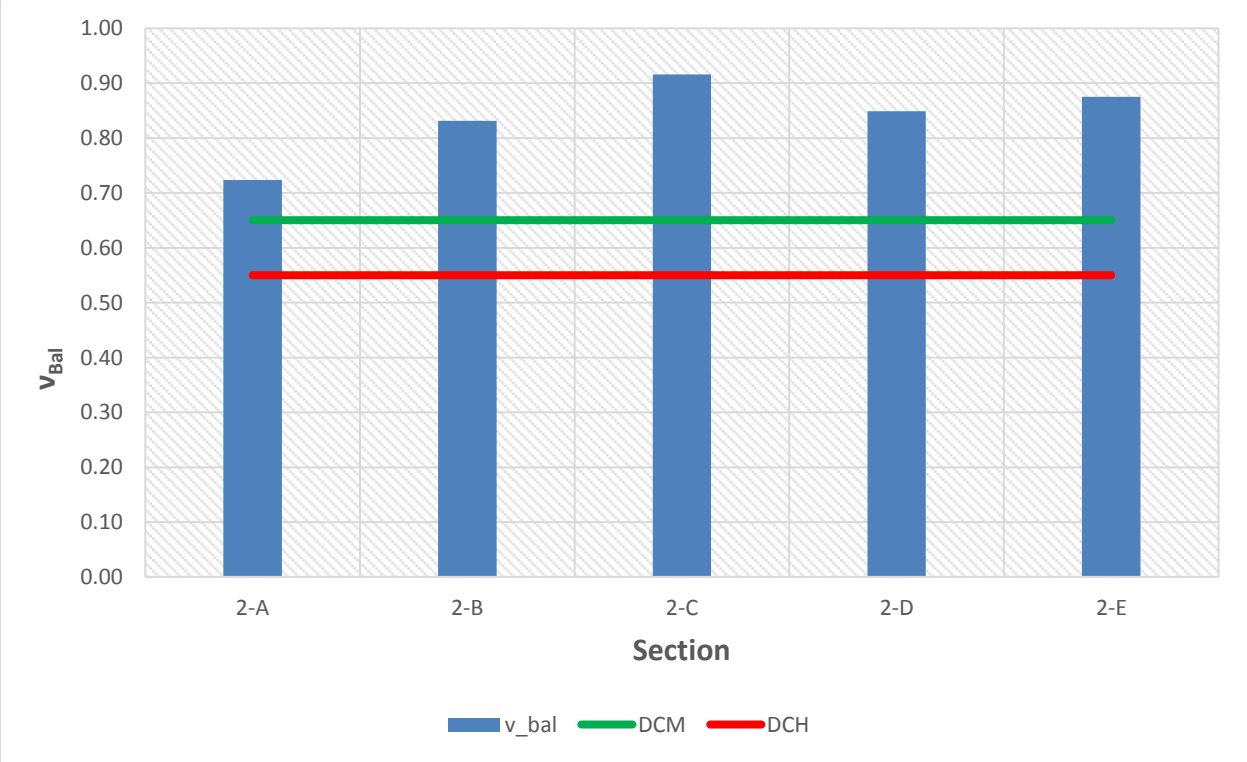

Figure 4-7: Normalised Balanced Load for Case -2

- **Case 3: Section 3-A to 3-E**

For the last group, ω is varied, while both ω_ω and δ_1 are kept relatively constant. Mechanical volumetric ratio of longitudinal reinforcement, ω, ranged from 0.17 for 3-A to 0.63 for 3-E. The results for Case-3 are summarised in Table 4.7 with Fig 4.8 showing their $v-\mu$ interaction charts. A similar trend is noticeable as in Section 4.2, shown in Annex B (Fig B.1 to B.10). It can be seen on Table 4.7 and Fig. 4.9, that there is a decrease in v_{bal} with an increase in ω. The resulting mean v_{bal} is 0.8002 with a coefficient of variation of 0.5%, which suggest v_{bal} not significantly affected by change in ω. However, balanced ultimate moment, $\mu_{u,Bal}$, of the section is highly increased by increasing ω. It has an average value of 0.3444 with a coefficient of variation of 24.3%. For the considered cross-sections $\mu_{u,Bal}$ has a range of $0.2523-0.4794$.

The results for the curvature properties are: φ_y averages at $6.26*10^{-6}\,rad/mm$ with coefficient of variation of 20.3%, the mean value of φ_u is $4.34*10^{-5}\,rad/mm$ with coefficient of variation of 18.1%, and finally curvature ductility has an average of 6.9687 with coefficient of variation of 3.9%. The conclusion from these results is that yield curvature, φ_y, ultimate curvature, φ_u, and curvature ductility, μ_φ, all are adversely affected by ω; all decreasing for increasing values of ω.

It is crucial to compare 2-A and 3-A, their only difference being the use of cross-ties for section 3-A. The curvature ductility enhanced from 3.3716 for 2-A to 6.8409 for 3-A, further emphasising with critical roles cross-ties and hoops have on ductility.

Table 4-7: Results of Case - 3

Section	3-A	3-B	3-C	3-D	3-E	Average	Coefficient of Variation
$\mu_{u,Bal}$	0.2523	0.3226	0.3956	0.2720	0.4794	**0.3444**	**24.3%**
$v_{u,Bal}$	0.7920	0.8033	0.8039	0.8014	0.8005	**0.8002**	**0.5%**
$\varphi_{u,Bal}$	5.68E-05	4.64E-05	4.18E-05	3.87E-05	3.35E-05	**4.34E-05**	**18.1%**
$\varphi_{y,Bal}$	8.30E-06	7.00E-06	6.06E-06	5.20E-06	4.76E-06	**6.26E-06**	**20.3%**
$\mu_{\varphi,Bal}$	6.8409	6.6248	6.8958	7.4432	7.0389	**6.9687**	**3.9%**

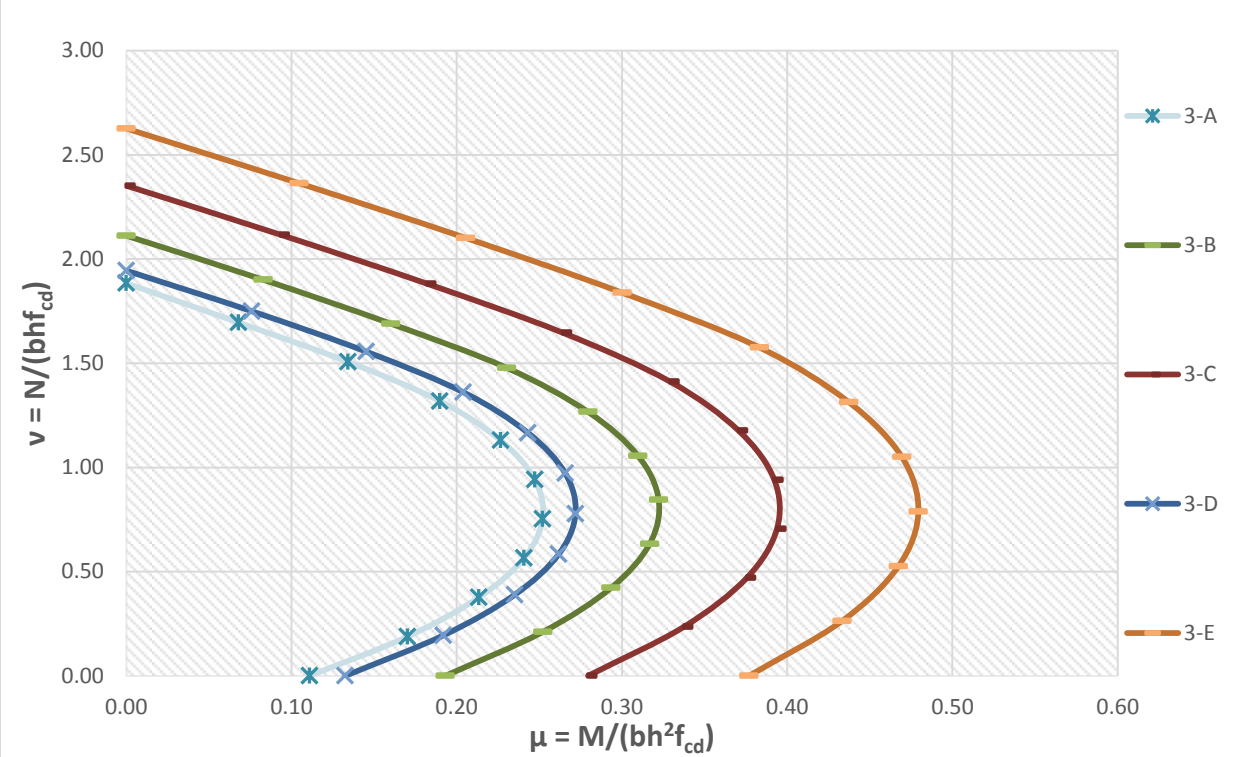

Figure 4-8: ν-μ Interaction for Case -3

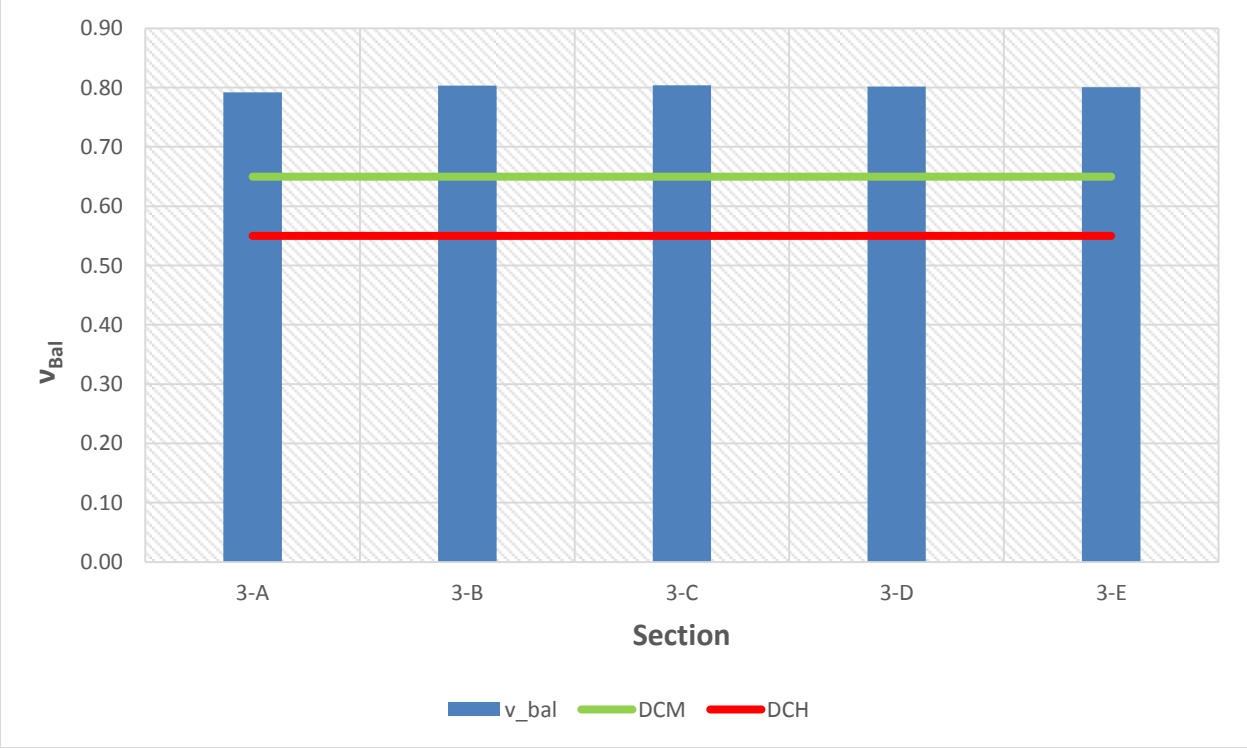

Figure 4-9: Normalised Balanced Load for Case -3

4.6. The Need for New Interaction Charts

As previously stated, the main reason behind the need for constructing a new interaction chart is the available design $\nu - \mu$ interaction chart on Design Aid ES-EN 1992:2015, as the name implies, is used for designing purposes. Therefore, it is more conservative to use for the purposes of researching the actual resisting capacity of an RC column sections. This is primarily because the design interaction chart uses the design strength and properties of both materials, i.e., concrete and reinforcements.

Another reason for the new proposed charts happens to be the new charts take into account the enhancing effects of transverse confinements on the concrete core. While the design chart doesn't do such a thing.

The last difference between these two charts is the normalising property utilized. For instance, the design charts normalise distance of the compression reinforcement from the extreme compression fibres, h_1 notified as d_1 in this paper, to the depth of the cross-section ($\delta_1 = h_1/h = d_1/h$). On the other hand, the charts presented here normalise d_1 to the effective depth of the cross-section ($\delta_1 = d_1/d$).

So, if the fore mentioned difference were to be made the same, the new interaction chart will yield similar charts depicted in the design aid of ES-EN 1992:2015.

4.7. Comparison of New chart Vs Design chart of ES-EN 1992:2015

Now that the reason for the new chart is mentioned, let us investigated the effects of the stated parameter when compared to the interaction charts depicted on the Design aid of ES-EN 1992:2015.

To go about doing such a task, lets pick 5 sections form the case studies of Section 4.4. The sections are selected to match the charts on the design aid. Once the sections are selected the comparison is done on the values of the normalized balanced failure load; designated as ν_{bal_ES} for ES EN 1992:2015 charts, and ν_{bal_New} for loads on the new charts.

Table 4-8: Comparison of New chart to ES-EN 1992:2015's chart

Section	ν_{bal_EC}	ν_{bal_New}	$\nu_{bal\_EC}/\nu_{bal\_NEW}$
1-A	0.467	0.7402	**0.631**
1-C	0.450	0.5793	**0.777**
1-E	0.465	0.9482	**0.490**
3-C	0.466	0.8014	**0.581**
3-E	0.466	0.8005	**0.582**

It can be concluded from Table 4-8, that the axial at balanced failure is increased by considering the parameters listed on Section 4.5. This is especially true for the effects of transverse confinements, ω_ω, has on the concrete core. It can also be noted that the balanced load is also influenced by the distance of compression reinforcement from the extreme compression fibres.

CHAPTER 5: CONCLUSION AND RECOMMENDATIONS

5.1. Conclusion

One of the aims of this research was to identify any limits on normalised axial load ratio set by major seismic code and compare these limits with ones stipulated in ES EN 1998:2015. The second objective was to explore the origins of the limiting requirements on ES EN 1998:2015 for the two ductility classes (DCM and DCH).

Six modern seismic codes were considered for the comparison, they were ES-EN 1998:2015, Eurocode 8, GB 50011-2010, ACI 318-11, NZS 3101.1.2006, and Hong Kong Concrete 2013. It was observed a lack of common consensus on limiting normalized axial loads among these codes. The first three codes do have explicitly stipulated limits on normalized axial loads in terms of design concrete strength of a section only, however, their values are not the same. Although the latter three codes do not directly limit normalized axial load, they do have limits on the maximum compressive loads allowed. These allowable maximum loads take into consideration both the strength of concrete and the reinforcement of the cross-section. It is also worth mentioning all the codes considered in this study have differing load combinations and their own sets of rules for column detailing.

It was also found the limits set by ES-EN 1998:2015 and Eurocode 8 are intended to ensure ductile failure. In other words, the limits are the upper and lower bound of balanced load observed from $P - M$ interaction charts.

To investigate where the balanced load would happen, a series of normalised $\nu - \mu$ interaction charts were constructed. These charts utilize the characteristic of both concrete and reinforcing steel. Confining effect of transverse reinforcement was also considered. The charts were calculated for two parameters: normalised distance of compression reinforcement from the extreme compression fibres with respect to effective depth, δ_1, and mechanical reinforcement ratios, ω. Fifteen different column cross-sections were also included as additional example case studies.

It is concluded from the results of the $v - \mu$ charts that the axial compressive load at balanced failure, v_{bal}, is highly dependent on the value of δ_1. Balanced load and δ_1 have an inversely proportional relationship. The obtained v_{bal} was greater than 0.65 for sections having values of δ_1 up to 0.15, for confinement complying with the minimum requirement of ES-EN 1998:2015 of DCM. While for sections confined in alignment with DCH confinements, it was found that v_{bal} was greater than 0.55 for all values of δ_1. The balanced load was also found to be inversely proportional to mechanical reinforcement ratios, ω, i.e. v_{bal} decreasing with increasing ω. The balanced load of a column section was enhanced by providing proper confinements, expressed in this paper by the mechanical volumetric ratio of confining reinforcement, ω_ω.

The results of the fifteen example case studies were found to be in alignment with the $v - \mu$ charts. Observations from these example cases are; the need for web reinforcement in between each corner bar in columns, and the advantage of utilizing cross-ties or hoops for confinements.

The results shown in this paper suggest, the limits set by ES-EN 1998:2015 can be more directed for specified values of δ_1. This is especially the case for column sections having lower values of δ_1, as these columns have higher balanced axial load v_{bal} higher than the required limits.

5.2. Recommendations

This research was limited to exploring the effect of axial compressive load on a cross-sectional level. Further researches should examine axial load effects on a member level, taking in o account slenderness and $P - \Delta$ effects. Actual lab experiments on a model-sized column would also be helpful for studying the numerous interacting properties such as; cracking and confinement, crack formation and bond deterioration, axial load and drift ductility, etc. Finally, behaviour of columns under cyclic loading conditions also needs further research.

REFERENCES

1. Fardis, M.N., *Seismic design, assessment and retrofitting of concrete buildings: based on EN-Eurocode 8*. Vol. 8. 2009: Springer.
2. Ministry of Construction, *ES EN 1998:2015: Design of structures for earthquake resistance-part 1: general rules, seismic actions and rules for buildings*, in *ES EN 1998:2015: Part 8-1*. 2015.
3. Code, Price,, *Eurocode 8: Design of structures for earthquake resistance-part 1: general rules, seismic actions and rules for buildings*. 2005, Brussels: European Committee for Standardization.
4. American Concrete Institute Committee, *Building code requirements for structural concrete (ACI 318-08) and commentary*. 2008, American Concrete Institute.
5. Paulay, T. and M.N. Priestley, *Seismic design of reinforced concrete and masonry buildings*. Vol. 768. 1992: Wiley New York.
6. Yuen, T.Y., J. Kuang, and V. Kobya, *Influence of Axial Compression Ratio on Drift Capacity of RC Columns.*
7. Yuen, T.Y., J.S. Kuang, and D.Y. Ho, *Ductility design of RC columns. Part 1: consideration of axial compression ratio.* HKIE TRANSACTIONS, 2016. **23**(4): p. 230-244.
8. Yuen, T.Y. and J. Kuang, *Revisiting the effect of axial force ratio on the seismic behaviour of RC building columns.* Structural Engineering International, 2017. **27**(1): p. 88-100.
9. Yuen, Y. and J.S. Kuang. *Axial compression effect on ductility design of RC structural walls*. in *2nd European Conference on Earthquake Engineering and Seismology*. 2014.
10. Fu, J., et al. *Effect of axial load ratio on seismic behavior of interior beam–column joints*. in *Proc. 12th world conf. earthquake eng*. 2000.
11. Matamoros, A., L. Matchulat, and C. Woods. *Axial load failure of shear critical columns subjected to high levels of axial load*. in *Proc. 14th World Conf. Earthq. Eng, Citeseer*. 2008. Citeseer.

12. Standards New Zealand, *Concrete structure standard-the design of concrete structures incorporating amendment No. 1 & 2 (NZS 3101: Part 1: 2006-A1&A2)*. 2006, SNZ Wellington, New Zealand.
13. Ministry of Construction of the People's Republic of China, *GB 50011-2010: Code for Seismic Design of Buildings*. 2010, Architecture & Building Press Beijing, China: Beijing.
14. CoP, H.K., *Code of Practice for Structural Use of Concrete*. 2013, Buildings Department , Hong Kong.
15. Code, Price,, *Eurocode 2: design of concrete structures-part 1–1: general rules and rules for buildings*. 2005, Brussels: European Committee for Standardization.
16. Ministry of Construction of the People's Republic of China, *GB 50010-2010: Code for Design of Concrete Structures*. 2010, China Architecture & Building Press: Beijing.
17. Penelis, G.G. and G.G. Penelis, *Concrete buildings in seismic regions*. 2014: CRC Press Boca Raton, FL, USA.

ANNEX A: ULTIMATE MOMENT RESISTANCE

The moment resistance of the confined core and of the un-spalled section, M_{Ro}, M_{Rc}, respectively, for use in $Eq(A.7a)$, may be estimated as uniaxial moment resistances of concrete sections with rectangular compression zone, for the Ultimate Limit State of such sections under uniaxial bending with axial force. The actual (or expected) value of material strengths is used, instead of the design values:

- for reinforcing steel, use f_{yk} in lieu of $f_{yd} = f_{yk}/\gamma_s$;
- for concrete, instead of $f_{cd} = \alpha_{cc} f_{ck}/\gamma_c$, the value f_{ck} or f_{cm} should be used before spalling (for M_{Rc}), and the value $f_{c,c}$ or $f_{cm,c}$ for the confined concrete core after spalling (for M_{Ro})
- for the moment corresponding to rupture of the tension reinforcement at the full section before spalling (and to the ultimate curvature φ_{su}), or at the confined core afterwards (and to $\varphi_{su,c}$), the cross-sectional area of tension reinforcement should be taken equal to $A_{s1}\, f_{tk1}/f_{yk1}$ (i.e., ω_1 should be multiplied by f_{tk1}/f_{yk1}).

Definitions and Assumptions

The ultimate curvature, φ_u, and ultimate moment resistance, M_u, of a section is identified with a distinct change in the pattern of the moment-curvature response which is taken as 20% reduction of the maximum ever resisting moment.

- Equilibrium conditions are considered for a structure without taking into account its deformations (first-order theory).
- Plane cross sections vertical to the axis of a beam under bending continue to be plane and vertical to the deformed axis up to failure (Bernoulli concept). In this respect, strain distribution over a cross section continues to be linear up to failure.
- The following $\sigma - \varepsilon$ laws of the materials are adopted here:
    - Unconfined concrete has a parabolic $\sigma - \varepsilon$ law up to the ultimate strength of f_{ck} and the corresponding strain, ε_{c2}. Beyond that point the $\sigma - \varepsilon$ law is horizontal

until a strain $\varepsilon_c \leq \varepsilon_{cu}$. Then the compression zone contributes to the axial compressive force with a force equal to $\xi(bdf_{ck})(1 - \varepsilon_{c2}/3\varepsilon_c)$.

- After spalling, the confined concrete core has an enhanced strength f_c^* and ultimate strain $\varepsilon_{cu,c}$.
- The $\sigma - \varepsilon$ law of reinforcing steel is mentioned on Section 3.1.2.

- There is perfect bonding between steel rebars and concrete, that is, strains of concrete and steel at any point of a cross section are identical
- Concrete cannot carry tensile stresses

Using the plane section hypothesis, the nonlinear $\sigma - \varepsilon$ laws outlined above, and from moment equilibrium of the normal stresses acting on the section with respect to its centroid, taken to be at mid-distance between the tension and the compression reinforcement, the ultimate moment-curvature relation can be computed.

Depending on the value of the axial load acting on the section, the amount and location of longitudinal bars, the degree of confinement of the compression zone by transverse reinforcement, and failure mode may take place either of these: *Failure of the Full Section due to Rupture of Tension Reinforcement before Spalling of the Concrete Cover*, *Ultimate Moment Resistance at Spalling of the Concrete Cover* and finally *Ultimate Moment of the Confined Core, After Spalling of the Cover*. Each of these failure modes are discussed below.

Failure of the full section due to rupture of tension reinforcement before spalling of the concrete cover

For this condition to be true, the normalized distance of the compression reinforcement from the extreme compression fibres, $\delta_1 = d_1/d$, must meet the following condition:

$$\delta_1 \leq \frac{\varepsilon_{cu} - \varepsilon_{y2}}{\varepsilon_{cu} + \varepsilon_{su}} \qquad (A.1)$$

- ***Case 1:*** - If $Eq(A.1)$ is satisfied and the axial load ratio, v, satisfies the inequality of $Eq(A.2)$,

$$\frac{\delta_1\varepsilon_{su}+\varepsilon_{y2}-(1-\delta_1)\frac{\varepsilon_{co}}{3}}{\varepsilon_{su1}+\varepsilon_{y2}}+\omega_2-\omega_1\frac{f_{t1}}{f_{y1}}-\frac{\omega_v}{\varepsilon_{su1}+\varepsilon_{y2}}\left[\varepsilon_{su1}-\varepsilon_{y2}+0.5(\varepsilon_{su1}+\varepsilon_{shv})\left(1+\frac{f_{tv}}{f_{yv}}\right)\right]\equiv$$

$$v_{s,y2}\le v\le v_{s,c}\equiv\frac{\varepsilon_{cu}-\frac{\varepsilon_{co}}{3}}{\varepsilon_{cu}+\varepsilon_{su1}}+\omega_2-\omega_1\frac{f_{t1}}{f_{y1}}-\frac{\omega_v}{(1-\delta_1)(\varepsilon_{su1}+\varepsilon_{cu})}\Big[\delta_1(\varepsilon_{su1}+\varepsilon_{cu})-(\varepsilon_{su1}-$$

$$\varepsilon_{cu})+0.5(\varepsilon_{su1}+\varepsilon_{shv})\left(1+\frac{f_{tv}}{f_{yv}}\right)\Big] \qquad (A.2)$$

Then, the compression reinforcement is beyond yielding but not yet in strain-hardening while the tension reinforcement is at ultimate strength. Then the moment resistance of the section is:

$$\frac{M_{Rc}}{bd^2f_c}=(1-\xi)\left[0.5\xi-\frac{\varepsilon_{co}}{3\varepsilon_{su1}}\left(0.5-\xi+\frac{\varepsilon_{co}}{4\varepsilon_{su1}}(1-\xi)\right)\right]+0.5(1-\delta_1)\left(\omega_1\frac{f_{t1}}{f_{y1}}+\omega_2\right)+$$

$$\frac{\omega_v}{(1-\delta_1)}\Big\{(\xi-\delta_1)(1-\xi)+\frac{1}{3}\left(\frac{(1-\xi)\varepsilon_{yv}}{\varepsilon_{su1}}\right)^2+\left[0.25(1-\delta_1)-\left(1-\frac{\varepsilon_{shv}}{\varepsilon_{su1}}\right)\frac{(1-\xi)}{6}\right]\left(1-\frac{\varepsilon_{shv}}{\varepsilon_{su1}}\right)\left(\frac{f_{t1}}{f_{y1}}-$$

$$1\right)(1-\xi)\Big\} \qquad (A.3)$$

With ξ given by

$$\xi_{su}\approx\frac{(1-\delta_1)\left(v+\omega_1\frac{f_{t1}}{f_{y1}}-\omega_2+\frac{\varepsilon_{co}}{3\varepsilon_{su}}\right)+\left(1+\delta_1+0.5\left(1-\frac{\varepsilon_{shv}}{\varepsilon_{su1}}\right)\left(1+\frac{f_{tv}}{f_{yv}}\right)\right)\omega_v}{(1-\delta_1)\left(1+\frac{\varepsilon_{co}}{3\varepsilon_{su1}}\right)+\left(2+0.5\left(1-\frac{\varepsilon_{shv}}{\varepsilon_{su1}}\right)\left(1+\frac{f_{tv}}{f_{yv}}\right)\right)\omega_v} \qquad (A.4)$$

- ***Case 2:*** **-** If $v<v_{s,y2}$, the compression reinforcement is elastic while the tension reinforcement is at ultimate strength. Then the moment resistance of the section is:

$$\frac{M_{Rc}}{bd^2 f_c} = (1-\xi)\left[0.5\xi - \frac{\varepsilon_{co}}{3\varepsilon_{su1}}\left(0.5 - \xi + \frac{\varepsilon_{co}}{4\varepsilon_{su1}}(1-\xi)\right)\right] + 0.5(1-\delta_1)\left(\omega_1\frac{f_{t1}}{f_{y1}} + \omega_2\frac{\xi-\delta_1}{1-\xi}\frac{\varepsilon_{su1}}{\varepsilon_{y2}}\right) + \frac{\omega_v}{6(1-\delta_1)}\left\{\left[1-\delta_1+\xi\left(1-\frac{\varepsilon_{yv}}{\varepsilon_{su1}}\right)\right]\left[1+\frac{\xi-\delta_1}{1-\xi}\frac{\varepsilon_{su1}}{\varepsilon_{yv}}\right]\left[0.5(1-\delta_1) - (1-\xi)\frac{\varepsilon_{yv}}{\varepsilon_{su1}}\right] + \left[\frac{2(1-\delta_1)}{3} - \left(1-\frac{\varepsilon_{shv}}{\varepsilon_{su1}}\right)(1-\xi)\right]\left(1-\frac{\varepsilon_{shv}}{\varepsilon_{su1}}\right)\left(\frac{f_{tv}}{f_{yv}}-1\right)(1-\xi)\right\} \qquad (A.5)$$

Where the normalized neutral axis depth, ξ is the positive root of

$$\left[1+\frac{\varepsilon_{co}}{3\varepsilon_{su}} + \frac{\omega_v}{2(1-\delta_1)}\left(1+\frac{f_{tv}}{f_{yv}}\left(1-\frac{\varepsilon_{shv}}{\varepsilon_{su1}}\right) + \frac{\varepsilon_{shv}-3\varepsilon_{yv}}{\varepsilon_{su1}} - \frac{\varepsilon_{su1}}{\varepsilon_{yv}}\right)\right]\xi^2 - \left[1+v+\frac{2\varepsilon_{co}}{3\varepsilon_{su}} + \omega_1\frac{f_{t1}}{f_{y1}} + \omega_2\frac{\varepsilon_{su1}}{\varepsilon_{y2}} + \frac{\omega_v}{(1-\delta_1)}\left(1+\frac{f_{tv}}{f_{yv}}\left(1-\frac{\varepsilon_{shv}}{\varepsilon_{su1}}\right) + \frac{\varepsilon_{shv}-3\varepsilon_{yv}}{\varepsilon_{su1}} - \delta_1\frac{\varepsilon_{su1}}{\varepsilon_{yv}}\right)\right]\xi + \left[v+\frac{\varepsilon_{co}}{3\varepsilon_{su}} + \omega_1\frac{f_{tv}}{f_{yv}} + \omega_2\delta_1\frac{\varepsilon_{su}}{\varepsilon_{y2}} + \frac{\omega_v}{2(1-\delta_1)}\left(1+\frac{f_{tv}}{f_{yv}}\left(1-\frac{\varepsilon_{shv}}{\varepsilon_{su1}}\right) + \frac{\varepsilon_{shv}-3\varepsilon_{yv}}{\varepsilon_{su1}} - \delta_1^2\frac{\varepsilon_{su1}}{\varepsilon_{yv}}\right)\right] = 0 \qquad (A.6)$$

Case 3: - If $Eq(A.1)$ is false, but v is still less than $v_{s,c}$ given on right hand side of $Eq(A.2)$, then the compression reinforcement is still elastic while the tension reinforcement is at ultimate strength. Then M_{Rc} of the section is again given by $Eq(A.1)$, with ξ from $Eq(A.2)$.

For the above three cases, means failure of the full section due to rupture if tension reinforcement before spalling of the concrete cover, the ultimate curvature, φ_{su}, is given by $Eq(3.16)$.

Ultimate Moment Resistance at Spalling of the concrete cover

For a limited range of axial load ratio, $v > v_{s,c}$, the concrete cover will spall before the tension reinforcement ruptures, but with the compression reinforcement already beyond yielding

When the outermost fibres reach the crushing strain of unconfined concrete, ε_{cu}, and the concrete cover spalls, the moment resistance of the section temporarily drops.

$$\text{If: } M_{Ro} \leq 0.8M_{Rc} \qquad (A.7a)$$

spalling of cover can be taken as the ultimate condition of the section. Where; M_{Rc} is the moment resistance of the full un-spalled section, and M_{Ro} is the moment resistance of the confined core of the section after spalling of the concrete cover as described in sub section *Ultimate Moment of the Confined Core, After Spalling of the Cover*.

There exists a range of ξ values for which both tension and compression reinforcement have yielded before ε_{cu} is reached at the extreme compression fibres, if

$$\delta_1 \leq \frac{\varepsilon_{cu}-\varepsilon_{y2}}{\varepsilon_{cu}+\varepsilon_{y1}} \qquad (A.3a)$$

is true. However, if $Eq(A.8a)$ is not met, range of ξ values exists where both the tension and the compression reinforcement will still be elastic when the extreme compression fibres reach a strain of ε_{cu}. The latter case results in a brittle behaviour of the cross section. As a result, two distinct cases are considered:

Case I: **-** If $Eq(A.8a)$ is met, is the more common and desirable in practice. Consider the equation below

$$\omega_2 - \omega_1 + \frac{\omega_v}{(1-\delta_1)}\left(\delta_1 \frac{\varepsilon_{cu}+\varepsilon_{y2}}{\varepsilon_{cu}-\varepsilon_{y2}} - 1\right) + \delta_1 \frac{\varepsilon_{cu}-\frac{\varepsilon_{co}}{3}}{\varepsilon_{cu}-\varepsilon_{y2}} \equiv v_{c,y2} \leq v \leq v_{c,y1} \equiv$$
$$\omega_2 - \omega_1 + \frac{\omega_v}{(1-\delta_1)}\left(\frac{\varepsilon_{cu}-\varepsilon_{y1}}{\varepsilon_{cu}+\varepsilon_{y1}} - \delta_1\right) + \frac{\varepsilon_{cu}-\frac{\varepsilon_{co}}{3}}{\varepsilon_{cu}+\varepsilon_{y1}} \qquad (A.9)$$

- ***Case 4:*** - If $Eq(A.8a)$ is met and if $v < v_{c,y2}$, the compression reinforcement is elastic while the tension reinforcement is beyond yielding but not yet in strain-hardening. With ξ given by positive root of $Eq(A.11)$, the moment resistance of the section is:

$$\frac{M_{Rc}}{bd^2 f_c} = \xi\left[0.5(1-\xi) - \frac{\varepsilon_{co}}{3\varepsilon_{cu}}\left(0.5 - \xi + \frac{\varepsilon_{co}}{4\varepsilon_{cu}}\xi\right)\right] + 0.5(1-\delta_1)\left(\omega_1 + \omega_2\frac{\xi-\delta_1}{\xi}\frac{\varepsilon_{cu}}{\varepsilon_{y2}}\right) + \frac{\omega_v}{4(1-\delta_1)}\left[\xi\left(1+\frac{\varepsilon_{yv}}{\varepsilon_{cu}}\right) - \delta_1\right]\left[1 + \frac{\varepsilon_{cu}}{\varepsilon_{yv}}\left(\frac{\xi-\delta_1}{\xi}\right)\right]\left[1 - \frac{\delta_1}{3} - \frac{2}{3}\xi\left(1+\frac{\varepsilon_{yv}}{\varepsilon_{cu}}\right)\right] \quad (A.10)$$

$$\left[1 + \frac{\varepsilon_{co}}{3\varepsilon_{su}} + \frac{\omega_v}{2(1-\delta_1)}\frac{(\varepsilon_{cu}-\varepsilon_{yv})^2}{\varepsilon_{cu}\varepsilon_{yv}}\right]\xi^2 + \left[v + \omega_1 + \omega_2\frac{\varepsilon_{cu}}{\varepsilon_{y2}} + \frac{\omega_v}{(1-\delta_1)}\left(1 + \delta_1\frac{\varepsilon_{cu}}{\varepsilon_{yv}}\right)\right]\xi - \left[\frac{\omega_2}{\varepsilon_{y2}} - \frac{\omega_v\delta_1}{2(1-\delta_1)\varepsilon_{yv}}\right]\varepsilon_{cu}\delta_1 = 0 \quad (A.11)$$

- ***Case 5:*** - If $Eq(A.8a)$ is satisfied and the axial load ratio, v, satisfies the inequality of $Eq(A.9)$, the tension and the compression reinforcement are both beyond yielding but not in strain-hardening. The moment resistance of the section by $Eq(A.13)$ with ξ taken as $Eq(A.13)$:

$$\frac{M_{Rc}}{bd^2 f_c} = \xi\left[0.5(1-\xi) - \frac{\varepsilon_{co}}{3\varepsilon_{cu}}\left(0.5 - \xi + \frac{\varepsilon_{co}}{4\varepsilon_{cu}}\xi\right)\right] + 0.5(1-\delta_1)(\omega_1+\omega_2) + \frac{\omega_v}{(1-\delta_1)}\left[(\xi-\delta_1)(1-\xi) - \frac{1}{3}\left(\frac{\xi\varepsilon_{yv}}{\varepsilon_{cu}}\right)^2\right] \quad (A.12)$$

$$\xi_{cu} = \frac{(1-\delta_1)(v+\omega_1-\omega_2) + (1+\delta_1)\omega_v}{(1-\delta_1)\left(1+\frac{\varepsilon_{co}}{3\varepsilon_{cu}}\right) + 2\omega_v} \quad (A.13)$$

- ***Case 6:*** - If $Eq(A.8a)$ is satisfied and the $v > v_{c,y1}$, the tension reinforcement is elastic while the compression reinforcement is beyond yielding but not in strain-hardening. With ξ from the positive root of $Eq(A.15)$, the moment resistance is:

$$\frac{M_{Rc}}{bd^2 f_c} = \xi\left[0.5(1-\xi) - \frac{\varepsilon_{co}}{3\varepsilon_{cu}}\left(0.5 - \xi + \frac{\varepsilon_{co}}{4\varepsilon_{cu}}\xi\right)\right] + 0.5(1-\delta_1)\left(\omega_1\frac{1-\xi}{\xi}\frac{\varepsilon_{cu}}{\varepsilon_{y1}} + \omega_2\right) + \frac{\omega_v}{4(1-\delta_1)}\left[1 - \xi\left(1-\frac{\varepsilon_{yv}}{\varepsilon_{cu}}\right)\right]\left[\frac{1}{3} - \delta_1 - \frac{2}{3}\xi\left(1-\frac{\varepsilon_{yv}}{\varepsilon_{cu}}\right)\right] \quad (A.14)$$

$$\left[1-\frac{\varepsilon_{co}}{3\varepsilon_{su}}-\frac{\omega_v}{2(1-\delta_1)}\frac{(\varepsilon_{cu}-\varepsilon_{yv})^2}{\varepsilon_{cu}\varepsilon_{yv}}\right]\xi^2+\left[\omega_1+\omega_2\frac{\varepsilon_{cu}}{\varepsilon_{y1}}-v+\frac{\omega_v}{(1-\delta_1)}\left(\frac{\varepsilon_{cu}}{\varepsilon_{yv}}-\delta_1\right)\right]\xi-\left[\frac{\omega_1}{\varepsilon_{y1}}+\frac{\omega_v}{2(1-\delta_1)\varepsilon_{yv}}\right]\varepsilon_{cu}=0 \quad (A.15)$$

Case II: - If $Eq(A.8a)$ is not met, which is a rare case. Consider the equation below

$$\omega_2\left((1-\delta_1)\varepsilon_{cu}-\delta_1\varepsilon_{y1}\right)-\omega_1+\frac{\omega_v}{2\varepsilon_{yv}}\left(\varepsilon_{cu}-\frac{1+\delta_1}{1-\delta_1}\right)+\frac{\varepsilon_{cu}-\frac{\varepsilon_{co}}{3}}{\varepsilon_{cu}+\varepsilon_{y1}}\equiv\bar{v}_{c,y1}\le v\le\bar{v}_{c,y2}\equiv\omega_2-\frac{\omega_1}{\varepsilon_{y1}}\frac{(1-\delta_1)\varepsilon_{cu}-\varepsilon_{y2}}{\delta_1}+\frac{\omega_v}{\delta_1\varepsilon_{yv}}\left(\frac{1+\delta_1}{1-\delta_1}\varepsilon_{y2}-\varepsilon_{cu}\right)+\delta_1\frac{\varepsilon_{cu}-\frac{\varepsilon_{co}}{3}}{\varepsilon_{cu}+\varepsilon_{y2}} \quad (A.16)$$

- ***Case 7:*** - If $Eq(A.8a)$ is not met and if $v<\bar{v}_{c,y1}$, the compression reinforcement is elastic and the tension reinforcement is beyond yielding but not strain-hardening yet. The moment resistance of the section is given by $Eq(A.10)$, with ξ from $Eq(A.11)$.
- ***Case 8:*** - If $Eq(A.8a)$ is not satisfied and the axial load ratio, v, satisfies the inequality of $Eq(A.16)$, the entire reinforcement of the section is elastic and the moment resistance is:

$$\frac{M_{Rc}}{bd^2f_c}=\xi\left[0.5(1-\xi)-\frac{\varepsilon_{co}}{3\varepsilon_{cu}}\left(0.5-\xi+\frac{\varepsilon_{co}}{4\varepsilon_{cu}}\xi\right)\right]+\frac{(1-\delta_1)\varepsilon_{cu}}{2\xi}\left((1-\xi)\frac{\omega_1}{\varepsilon_{y1}}+(\xi-\delta_1)\frac{\omega_2}{\varepsilon_{y2}}\right)+\frac{\omega_v(1-\delta_1)^2}{12\xi}\frac{\varepsilon_{cu}}{\varepsilon_{yv}} \quad (A.17)$$

$$\left[1-\frac{\varepsilon_{co}}{3\varepsilon_{cu}}\right]\xi^2-\left[v-\left(\frac{\omega_1}{\varepsilon_{y1}}+\frac{\omega_2}{\varepsilon_{y2}}\mp\frac{\omega_v}{(1-\delta_1)\varepsilon_{yv}}\right)\varepsilon_{cu}\right]\xi-\left[\frac{\omega_1}{\varepsilon_{y1}}+\frac{\omega_2\delta_1}{\varepsilon_{y2}}+\frac{\omega_v(1+\delta_1)}{2(1-\delta_1)\varepsilon_{yv}}\right]\varepsilon_{cu}=0 \quad (A.18)$$

- ***Case 9:*** - If $Eq(A.8a)$ is not satisfied and the $v>\bar{v}_{c,y2}$, the tension reinforcement is elastic and the compression reinforcement is beyond yielding but not in strain-hardening. The moment resistance of the section is given by $Eq(A.14)$, with ξ from $(A.15)$.

For the above six cases the ultimate curvature, φ_{cu}, is given by (3.17).

Ultimate Moment of the Confined Core, After Spalling of the Cover

$$\text{If: } M_{Ro} > 0.8M_{Rc} \qquad (A.7b)$$

then the confined core of the section recovers from spalling of the concrete shell around it. It ultimately fails either by rupture of the tension reinforcement or by disintegration of the extreme compression fibres of the core itself.

All the pervious failure modes also apply where with the exception of *Case II*. These is because that d_{c1} is small compared to d_1, the conditions of $Eqs.\ (A.1)$, and $(A.8)$ are always met in the confined core. The following properties need to be adjusted to take in account the trigger of confinement

- dimensions b, d and d_1 are replaced by $b_c = b - 2 * \left(cover + \phi_{stirrup}/2\right)$, $d_c = d - \left(cover + \phi_{stirrup}/2\right)$ and $d_{c1} = \phi_{stirrup}/2 + \phi_{longtitudinal}/2$, respectively;
- $N, \rho_1, \rho_2, \rho_v$ are normalized to $b_c d_c$, instead of bd, and
- the $\sigma - \varepsilon$ parameters of confined concrete, f_c^*, ε_{cu}^*, are used, in lieu of f_c, ε_{cu}.

Then, only $Eqs.\ (A.2), (A.4), (A.6), (A.9), (A.13), (A.15)$, and $(A.11)$ in sub-sections the *Failure of the Full Section Due to Rupture of Tension Reinforcement Before Spalling of the Concrete Cove*r and *Moment Resistance at Spalling of the Concrete Cover* are meaningful for the normalized distance of neutral axis, ξ. The ultimate moment resistance of the confined core, M_{Ro}, after spalling of the cover will be obtained from $Eqs.\ (A.3), (A.5), (A.12), (A.14)$, and $(A.10)$, from their respective ξ.

ANNEX B: INTERACTION CHARTS

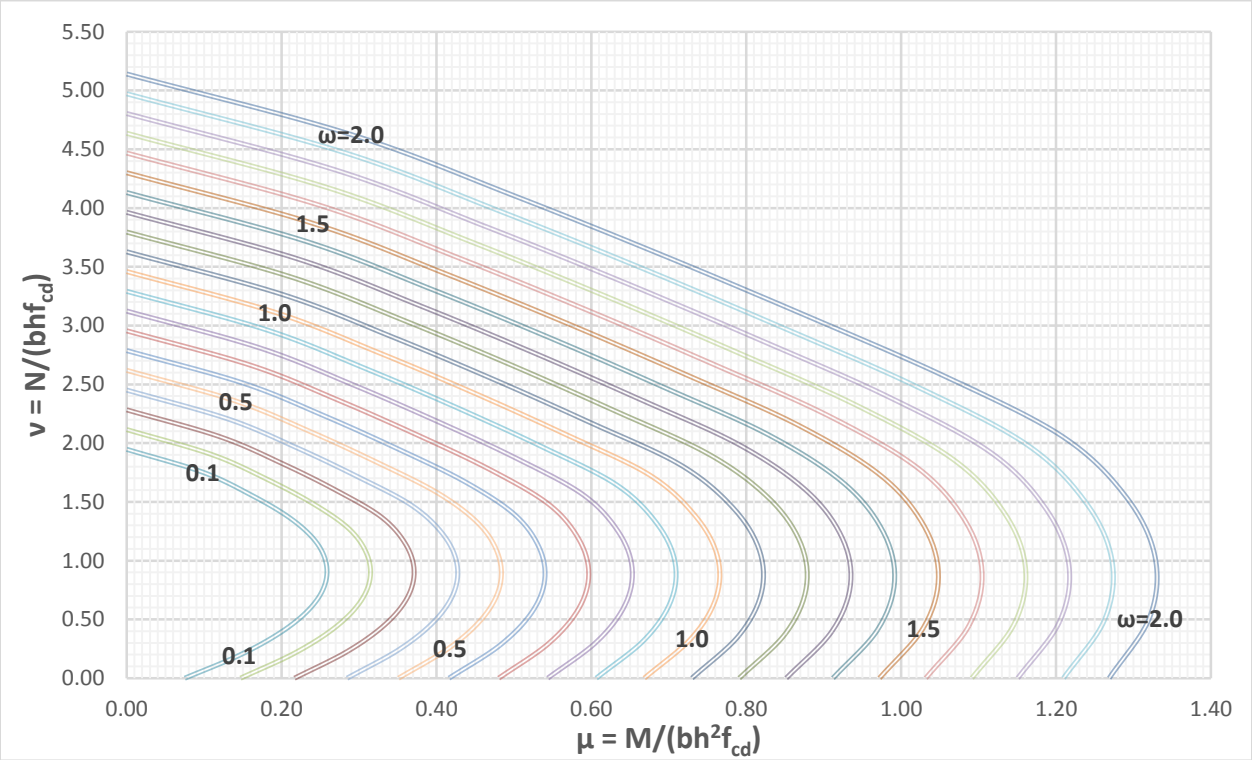

Figure B-1: ν-μ Interaction for δ_1=0.05 (DCM)

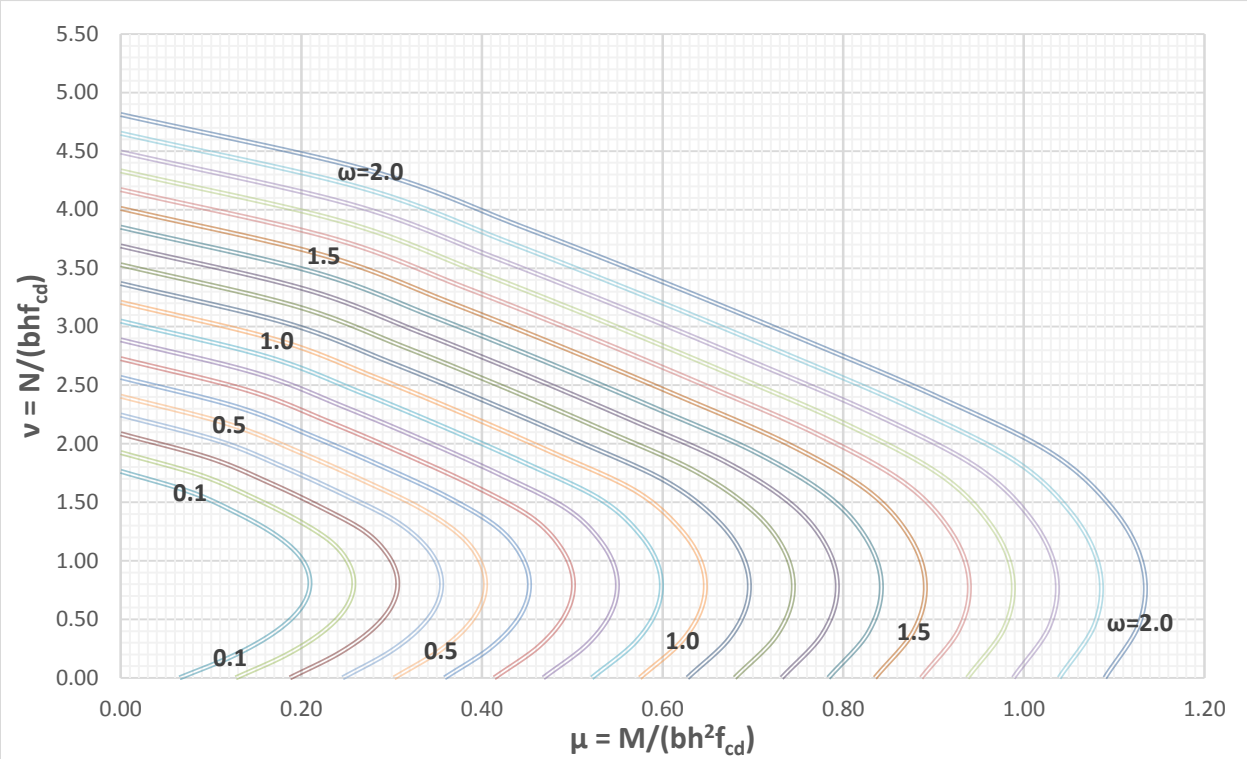

Figure B-2: ν-μ Interaction for δ_1=0.10 (DCM)

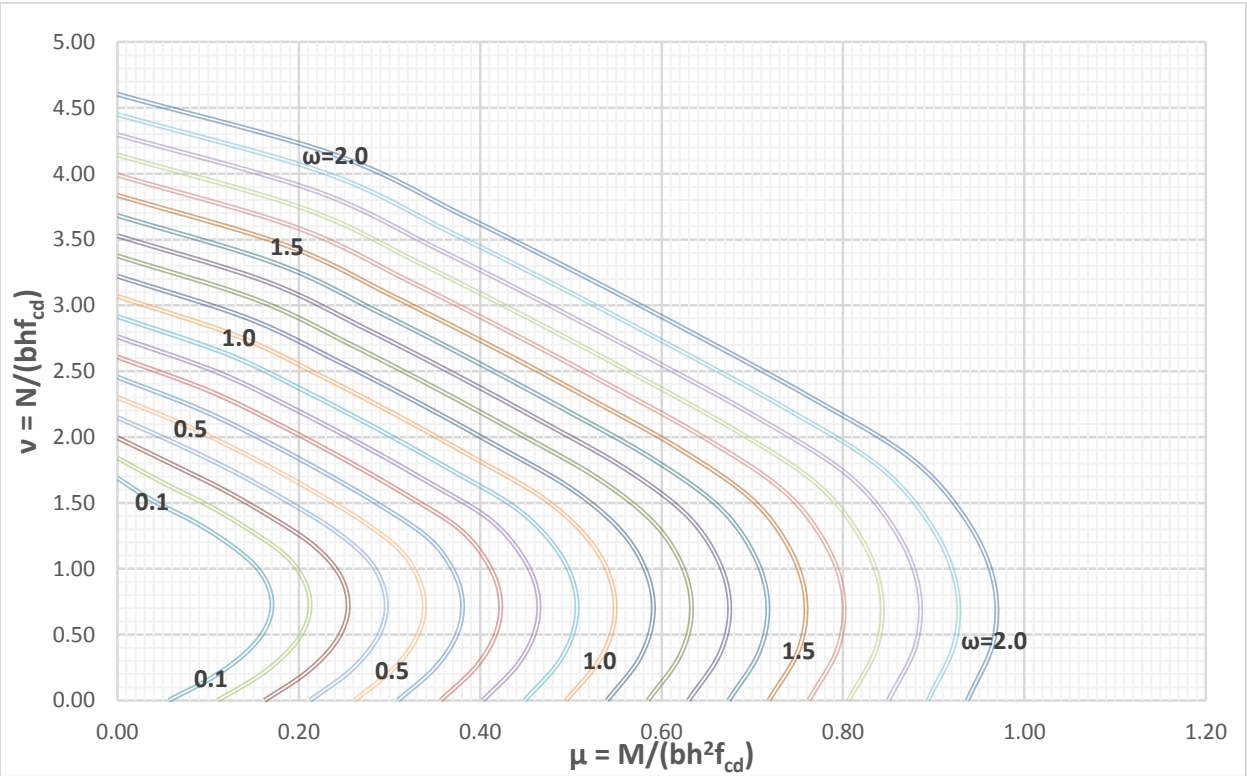

Figure B-3: ν-μ Interaction for δ_1=0.15 (DCM)

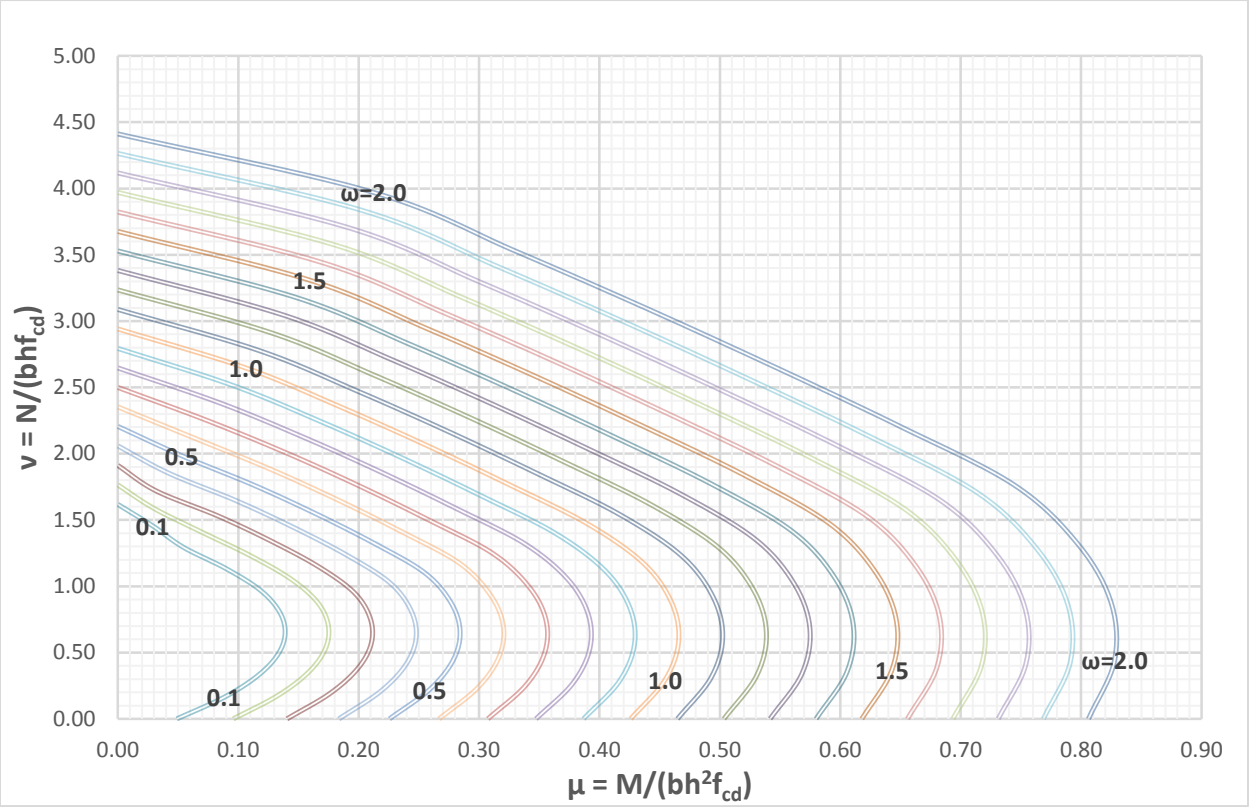

Figure B-4: ν-μ Interaction for δ_1=0.20 (DCM)

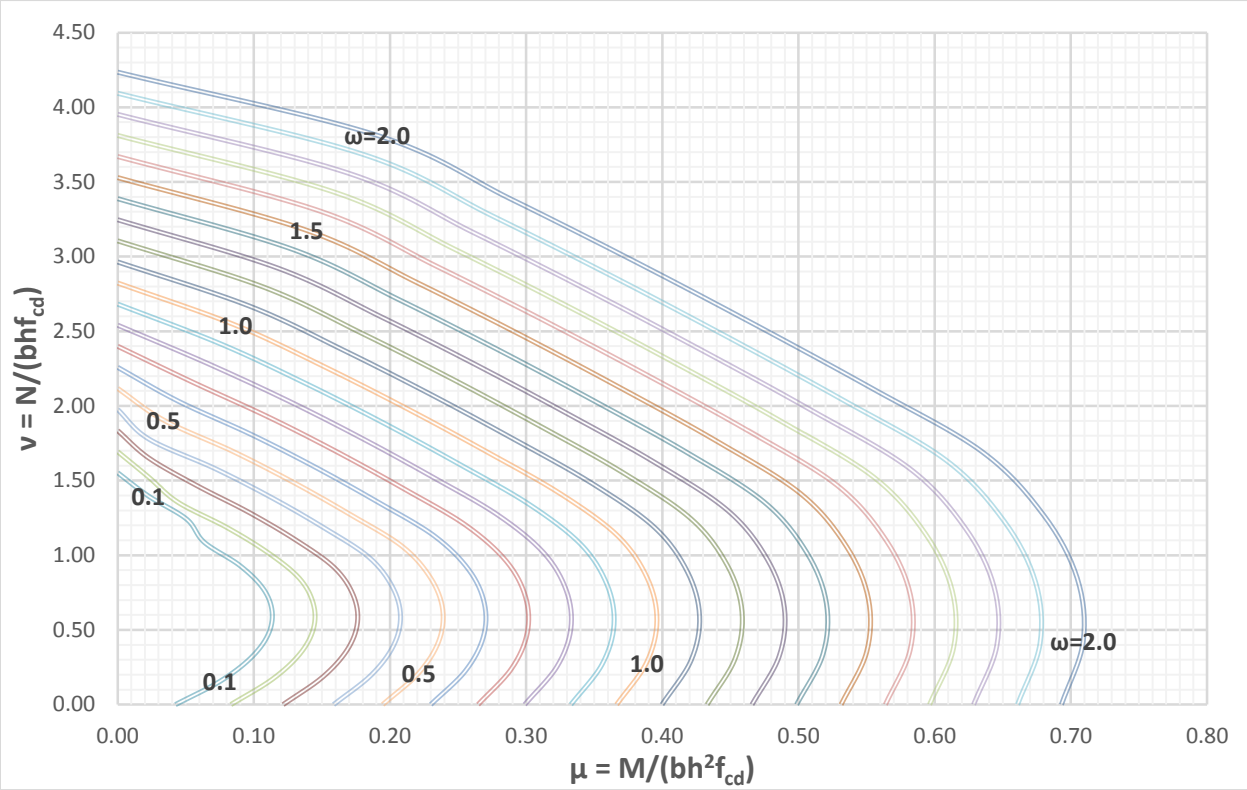

Figure B-5: ν-μ Interaction for δ_1=0.25 (DCM)

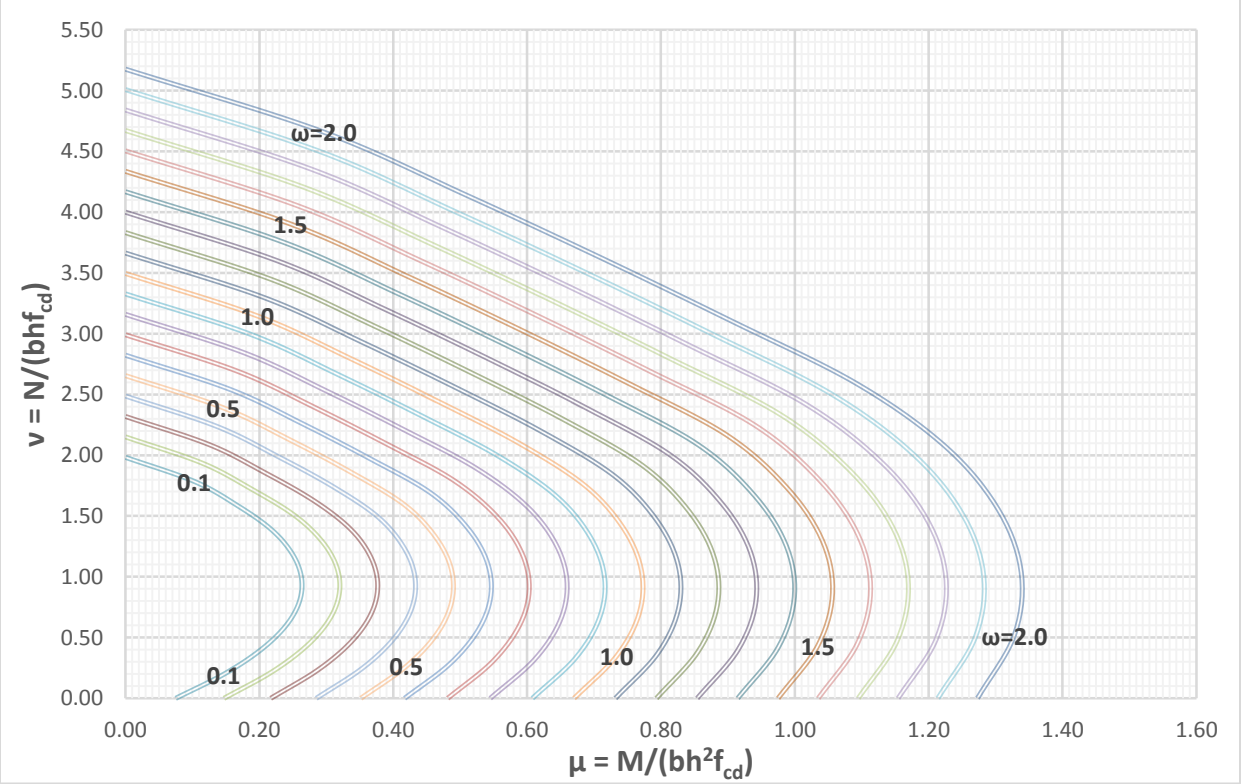

Figure B-6: ν-μ Interaction for δ_1=0.05 (DCH)

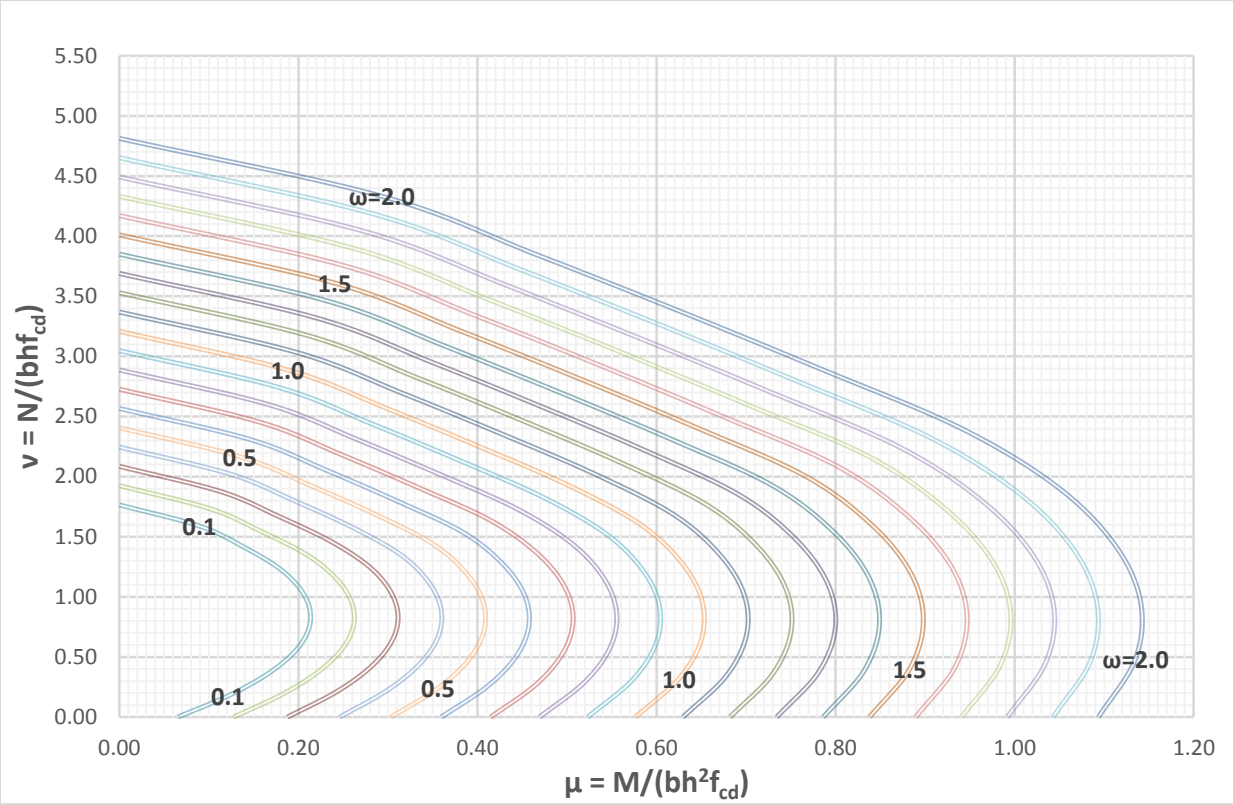

Figure B-7: ν-μ Interaction for δ_1=0.10 (DCH)

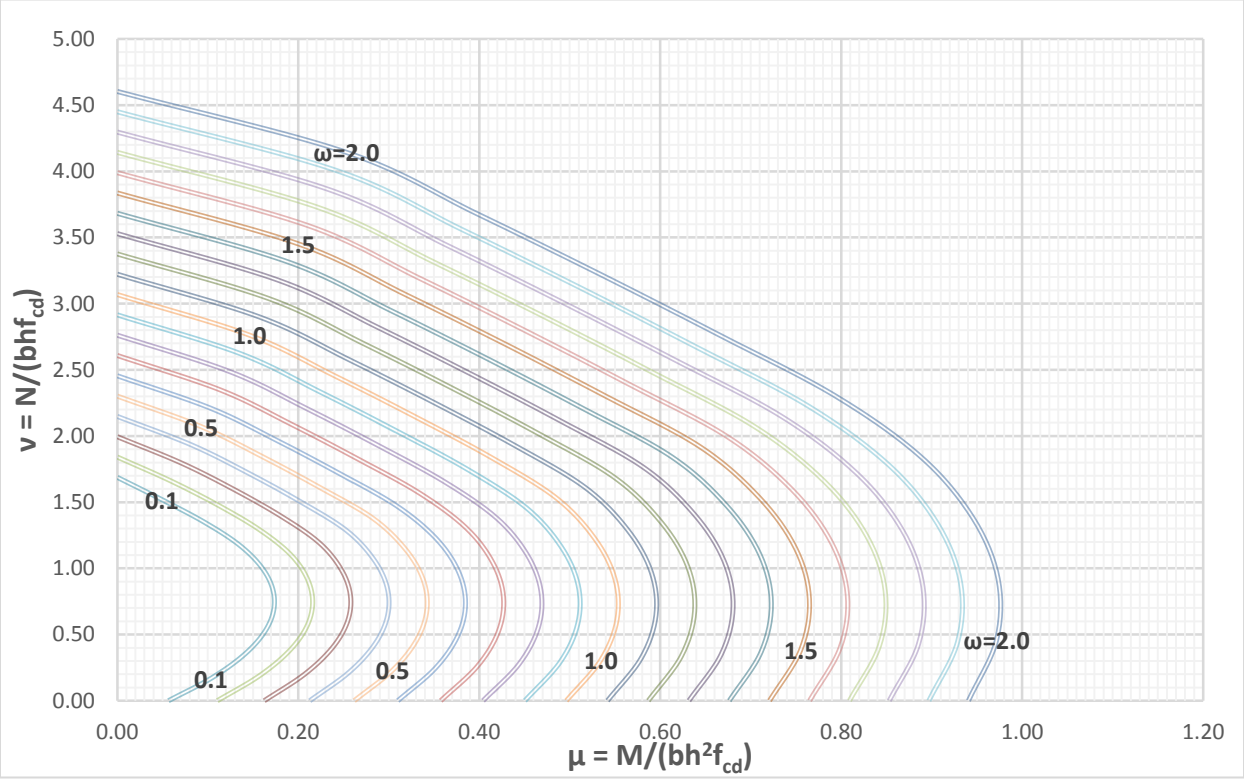

Figure B-8: ν-μ Interaction for δ_1=0.15 (DCH)

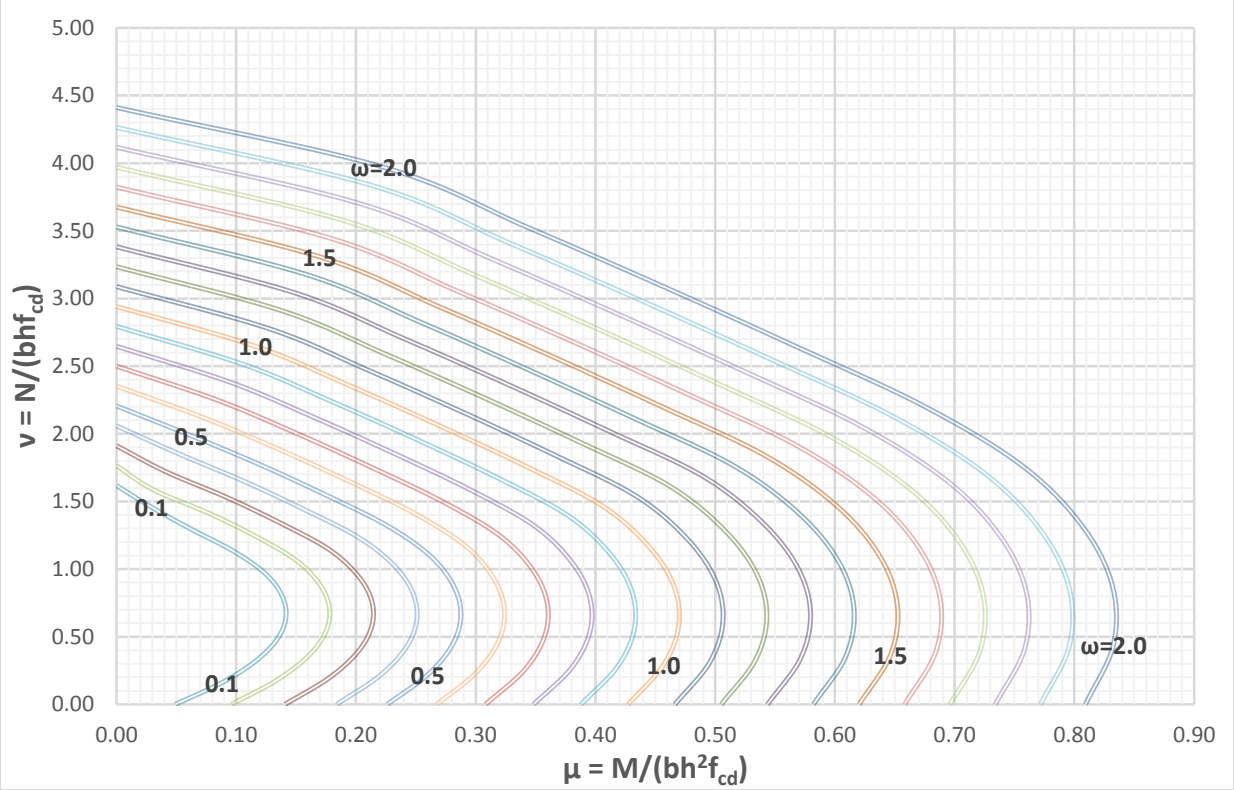

Figure B-9: ν-μ Interaction for δ_1=0.20 (DCH)

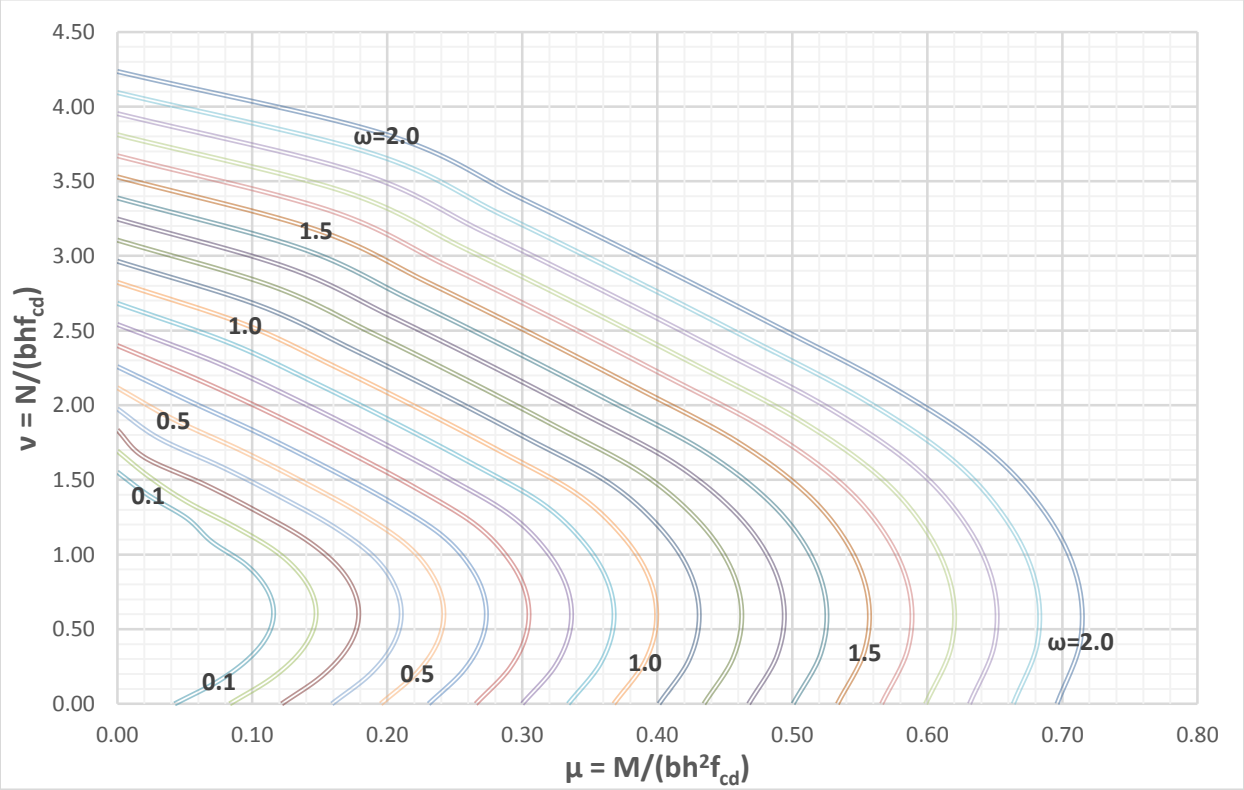

Figure B-10: ν-μ Interaction for δ_1=0.25 (DCH)